PHILOSOPHICAL TRANSACTIONS OF THE ROYAL SOCIETY A MATHEMATICAL, PHYSICAL & ENGINEERING SCIENCES

Grain Boundaries as Heterogeneous Systems: Atomic and Continuum Elastic Properties

I. Alber, J. L. Bassani, M. Khantha, V. Vitek and G. J. Wang

Phil. Trans. R. Soc. Lond. A 1992 **339**, 555-586
doi: 10.1098/rsta.1992.0051

Grain boundaries as heterogeneous systems: atomic and continuum elastic properties

By I. Alber[1], J. L. Bassani[1], M. Khantha[2], V. Vitek[2] and G. J. Wang[2]

[1] *Department of Mechanical Engineering and Applied Mechanics, and*
[2] *Department of Materials Science and Engineering, University of Pennsylvania, Philadelphia, Pennsylvania 19104, U.S.A.*

Contents

The relation between atomic structure and elastic properties of grain boundaries is investigated theoretically from both atomistic and continuum points of view. A heterogeneous continuum model of the boundary is introduced where distinct phases are associated with individual atoms and possess their atomic level elastic moduli determined from the discrete model. The effective elastic moduli for sub-blocks from an infinite bicrystal are then calculated for a relatively small number of atom layers above and below the grain boundary. These effective moduli can be determined exactly for the discrete atomistic model, while estimates from upper and lower bounds are evaluated in the framework of the continuum model. The complete fourth-order elastic modulus tensor is calculated for both the local and the effective properties. Comparison between the discrete atomistic results and those for the continuum model establishes the validity of this model and leads to criteria to assess the stability of a given grain boundary structure. For stable structures the continuum estimates of the effective moduli agree well with the exact effective moduli for the discrete model. Metastable and unstable structures are associated with a significant fraction of atoms (phases) for which the atomic-level moduli lose positive definiteness or even strong ellipticity. In those cases, the agreement between the effective moduli of the discrete and continuum systems breaks down.

Phil. Trans. R. Soc. Lond. A (1992) **339**, 555–586
Printed in Great Britain

1. Introduction

Grain boundaries and interfaces between dissimilar materials are domains of distinct atomic structure and, in the case of alloys, also composition. Consequently, the physical and chemical properties of interfacial regions are often very different from those of the bulk. Many of the physical properties of polycrystalline and/or composite materials are controlled by interfacial phenomena. For this reason studies of the atomic structure of grain boundaries and other interfaces have been in the forefront of materials research for a long time (see, for example, proceedings of recent conferences edited by Ishida (1986), Raj & Sass (1987), Yoo *et al.* (1988), Aucouturier (1990) and Rühle *et al.* (1990)). Theoretical analyses of the atomic structures of grain boundaries are now well developed but studies of more general interfaces are still rare. The main reason is the lack of physically justified descriptions of atomic interactions in the latter case (see, for example, Vitek & Srolovitz 1989; Tersoff *et al.* 1989; Rühle *et al.* 1990).

Until recently, the main aim of the majority of the atomistic studies of grain boundaries was to investigate the dominant structural features and their relation to geometrical, crystallographic, characteristics of grain boundaries (see, for example, reviews by Sutton (1984), Vitek (1984), Bristowe (1986), Balluffi (1986), Balluffi *et al.* (1987)). Examples are studies of the principal relaxation modes at boundaries, the relation between structures of various boundaries throughout a misorientation range, and the uniqueness and/or multiplicities of boundary structures. Understanding of the structural characteristics of grain boundaries is important in its own right, but the ultimate goal of atomistic studies is to uncover links between the atomic structure and properties of grain boundaries.

In this paper we explore the elastic properties of the grain boundary region. Several recent calculations, indeed, suggest that the elastic moduli in the boundary domain may differ significantly from those of the bulk. Wolf and co-workers (Wolf *et al.* 1989; Wolf & Lutsko 1989; Wolf & Kluge 1990), who examined superlattices of (001) twist boundaries, as well as Adams *et al.* (1989), who studied the $\Sigma = 5\,(001)$ twist boundary in a thin film of copper, find an increase of the Young's modulus perpendicular to the boundary plane and a substantial decrease of the shear modulus in the boundary plane in the atomic layers adjacent to the boundary. The main aim of this paper is to establish a rigorous characterization of the spatially varying elastic modulus tensor in the interfacial region consistent with the moduli that enter in local linear elasticity theory. Towards this end we develop a continuum analogue of grain boundaries in which the local variation of the elastic properties is fully accounted for in terms of distinct phases, and then analyse the overall or effective elastic properties of bicrystals within this heterogeneous continuum framework. As will be seen, this continuum analogue is, in turn, extremely useful for analysing the discrete atomistic results, for example, in distinguishing among locally stable, metastable and unstable structures for the same bicrystal.

For an ensemble of atoms in equilibrium for which the energy can be written as a unique function of atomic positions, the effective first-order and second-order elastic constants can be evaluated using the method of homogeneous deformations (Born & Huang 1954). This is described in more detail in §4 and in Appendix B. In the present case the ensemble is the block of atoms containing a planar interface in the middle of the block. The first-order elastic constants are, of course, identified with the internal stresses and the second-order elastic constants have the usual meaning of

moduli. In general, the (second order) elastic moduli consist of two parts: the homogeneous part and the relaxation part. The latter is related to the fact that in non-centrosymmetric systems of particles the response of individual particles to a macroscopically homogeneous applied strain is inhomogeneous (Born & Huang 1954; Martin 1975*a*, *b*). Given the structure of a discrete non-centrosymmetric system the overall or effective moduli, i.e. the homogeneous plus the relaxation parts, can be determined exactly. An analogous problem arises in a heterogeneous continuum, composed of phases with different elastic properties, subject to a uniform applied loading, although in this case obtaining exact solutions of the partial differential equations for arbitrary phase geometries (including polyhedral) becomes practically impossible. This is discussed in more detail in §3.

In discrete structures, the total energy of which can be written as a sum of energies associated with individual atoms, an important feature of the overall first-order elastic constants, i.e. internal stresses (or residual stresses if self equilibriated), and second-order elastic constants, i.e. moduli, is that they can be written as sums over all the atoms of the ensemble. Hence, we can identify, at least formally, both the stresses and the elastic moduli associated with individual atoms, i.e. at the position of individual atoms; these will be called atomic level stresses and elastic moduli. A similar approach has been adopted in studies of the structure and properties of glasses and liquids where atomic level stresses were used to analyse both the density and topological structural fluctuations (Srolovitz *et al.* 1981; Vitek & Egami 1987; Chen *et al.* 1988). The question as to whether this algebraic definition of local elastic properties is reasonable is partly answered through comparisons with the heterogeneous continuum models.

A continuum model of grain boundaries is conceived as a heterogeneous medium where different phases are identified with individual atoms. Each phase of the continuum is taken to occupy the interior of the Voronoi polyhedron of the corresponding atom and the elastic moduli associated with this atom are defined as the elastic moduli of this phase. Typically, in the region of the interface the elastic moduli are generally anisotropic, that is there are 21 distinct components for each atom. As explained in §3*b*, in the framework of local elasticity theory this model is physically meaningful if the elastic moduli of each phase are positive definite or, at least, meet the weaker condition of strong ellipticity (see, for example, Knops & Payne 1971).

Theoretical elasticity helps to guide the interpretation of the atomic level elastic moduli. If for a particular atom these moduli are positive definite, then upon deforming the entire block uniformly the energy change associated with that atom will be positive. Otherwise it could be negative, which at the continuum level, at least, is thought to be unusual. This is expanded upon below. If the moduli are at least strongly elliptic, then elastic waves in a solid possessing these moduli will propagate with real wave speeds.

By using the results of the atomistic studies it is shown here that positive definiteness is satisfied except for a very small number of atoms in the boundary. Whether or not the moduli of these atoms are strongly elliptic cannot always be readily determined, as discussed in §3*b*, although for some atoms it is found that the moduli certainly are not. When the elastic moduli of each phase (atom) are positive definite the classical uniform strain Voigt upper bound and the uniform stress Reuss lower bound on the effective or overall elastic moduli can be utilized (Willis 1981). Furthermore, if the moduli associated with individual atoms are at least strongly

PHILOSOPHICAL TRANSACTIONS OF THE ROYAL SOCIETY A MATHEMATICAL, PHYSICAL & ENGINEERING SCIENCES

elliptic then the Voigt upper bound still applies and a new lower bound, based on an extension of the recently developed translation method (Francfort & Murat 1986; Milton 1990), can be applied. Since for discrete structures the effective moduli can be evaluated exactly, in §5 we carry out a comparison between the bounds and the exact effective moduli for the boundaries studied. In most cases these bounds are really only estimates that behave like bounds since one or more of the phases (atoms) lose strong ellipticity.

This comparison between the discrete and continuum models provides an assessment of the validity of the continuum model in its ability to capture the actual behaviour of the interfacial region even when the thickness of this region is of the order of a few lattice parameters. At the same time, it also aids in evaluating the relative stability with respect to small perturbations, of different atomic structures of a particular crystallographically defined grain boundary, i.e. of different multiple structures (Wang *et al.* 1984). Three distinct cases have been found here. First are the structures for which the exact effective moduli lie between the continuum bounds (estimates). Such structures are locally stable in the sense that these structures persist after small perturbations. The second are boundaries with some effective moduli that lie below the lower bound. These structures are also not unstable but usually correspond to a higher total energy configuration than the first type; these will be termed 'metastable'. Finally, when some of the exact effective moduli lie above the upper bound the structure is not stable which indicates an inadequacy in relaxation even though the usual criteria for the termination of the relaxation process are satisfied (see §2). Nearly all the structures we have calculated are, in fact, stable. In the stable cases the continuum development presents an unambiguous definition of the interfacial elastic moduli that can be naturally adopted to describe bimaterial interfaces as well by formulating physically meaningful traction–displacement jump relations (see Bassani & Qu 1990). In this way continuum analyses of processes such as intergranular cracking and localized plastic flow near grain boundaries and of the effective response of heterogeneous solids can incorporate realistic descriptions of interfaces.

2. Atomistic models of grain boundaries

All the atomistic studies presented here have been carried out for grain boundaries in pure metals and the method of calculation was principally the same as in a number of previous studies (see, for example, Vitek *et al.* 1979; Sutton & Vitek 1983). First a block consisting of the atomic coordinates of an unrelaxed face centred cubic (FCC) bicrystal containing the chosen boundary is constructed in the computer using the geometrical rules of the coincidence site lattice (CSL). The periodicity imposed by the CSL in the boundary plane is then maintained throughout the relaxation process. A relaxed structure is found using a molecular statics method in which the total internal energy is minimized with respect to both the local atomic displacements and relative rigid body translations of the adjoining grains. This procedure allows for expansion and/or contraction perpendicular to the boundary plane but not parallel to the boundary. Thus in the relaxed configuration the average stress in the direction perpendicular to the boundary is zero but an average interfacial stress, corresponding to the tangential stress components in the boundary plane, remains (Ackland & Finnis 1986). This correctly reflects the constraints imposed upon the grain boundaries in both polycrystalline materials and large bicrystals.

The relaxation was regarded as complete when the force acting on any atom of the relaxed block did not exceed 10^{-3} eV Å^{-1}.† This is a somewhat arbitrary criterion but it was found in a number of previous calculations that a further decrease of the force did not lead to any significant change in the boundary structure and energy. However, it is shown here (§5) that this criterion is not entirely adequate and unstable structures may result in some cases. The analysis presented in this paper may then help to identify such cases.

The atomistic calculations carried out in this study have been made using the empirical Finnis–Sinclair type many-body potentials (Finnis & Sinclair 1984) to describe atomic interactions. A limited study was also performed using a Lennard–Jones truncated equilibrium pair-potential. However, the grain boundary structures calculated using these two different descriptions of interatomic forces have all been found to be very similar (see also Wolf *et al.* 1989). Thus the qualitative results are not sensitive to the details of the description of atomic interactions and we present here only the results for the many-body potentials (Ackland *et al.* 1987).

In the case of many-body potentials and/or the embedded atom method (Daw & Baskes 1983, 1984), which are equivalent approaches (Johnson 1988), the energy of an atom α is written as:

$$U_\alpha = \tfrac{1}{2}\sum_\beta V(R^{\alpha\beta}) - f(\rho^\alpha), \tag{2.1}$$

where $R^{\alpha\beta}$ is the separation of the atoms α and β and V is a pair potential which is strongly repulsive for small separations of atoms. f is the many body or embedding function which is taken as the square root in the Finnis–Sinclair scheme, and

$$\rho^\alpha = \sum_\beta \Phi(R^{\alpha\beta}), \tag{2.2}$$

where Φ is a short-range pair-potential which can be interpreted as a sum of squares of hopping integrals within the tight-binding approach incorporating charge conservation (Finnis & Sinclair 1984; Ackland *et al.* 1988). (The indicial notation adopted throughout this paper is as follows: Greek indices denote atoms or phases. Lower case Roman subscripts denote cartesian components of tensors. Summation over repeated Roman indices is implied using Einstein's convention while summation over Greek indices is indicated explicitly.) The summations extend over all the atoms β interacting with the atom α and the total energy of the system is then taken as the sum of energies of individual atoms. Both V and Φ are fitted empirically so as to reproduce the equilibrium crystal structure, elastic moduli, cohesive energy and vacancy formation energy of the given material. The many-body term in equation (2.1) allows us to include local density variations into the energy calculations which is important for studies of interfaces.

In the present work we have studied symmetrical tilt and twist boundaries with the [001] rotation axis and the corresponding crystallographic parameters of these boundaries are summarized in table 1. The natural interface coordinate system is always chosen with the x_3 axis taken to be perpendicular to the grain boundary (interface) and the x_1 and x_2 axes parallel to the boundary plane. In the case of tilt boundaries the tilt axis corresponds to the x_2 axis, whereas for the (001) twist

† 1 Å = 10^{-10} m = 10^{-1} nm.

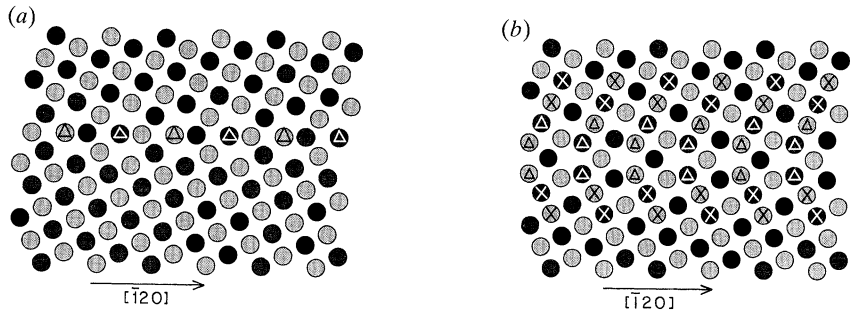

Figure 1. The relaxed structures of the $\Sigma = 5$ [001]/(210) symmetrical tilt boundary calculated using the many-body potential for gold. (*a*) B structure, (*b*) B′ structure. The atoms, projected in the [001] direction, are depicted as shaded circles, and two different shades represent atoms from two different (002) planes in the [001] period.

Table 1. *Crystallographic characteristics of grain boundaries studied*

Σ	misorientation	boundary plane
tilt boundaries		
5	37.87°	(210)
5	53.13°	(310)
13	22.62°	(320)
13	67.38°	(510)
73	48.89°	(830)
twist boundaries		
5	36.87°	(001)
13	22.62°	(001)
25	16.26°	(001)

boundaries x_2 (and also x_1), is taken parallel to one of the CSL vectors. The structures of all the boundaries studied are practically the same as those found in the previous works (Wang *et al.* 1984; Schwartz *et al.* 1985; Wang & Vitek 1986; Schwartz *et al.* 1988) and are not, therefore, presented here in detail. The analysis of the elastic moduli in the grain boundary region is presented in detail for the $\Sigma = 5$ (210) symmetrical tilt and $\Sigma = 5$ twist boundaries. For the other boundaries studied only the main features of the elastic moduli are described. Most results presented here were obtained using the potentials for gold, but for the $\Sigma = 5$ (210) boundary results obtained using the potentials for copper are also shown.

It should be noted that, as in former studies, more than one structure corresponding to local minima in total energy has been found for crystallographically equivalent boundaries (arrived at from different initial configurations). This structural multiplicity is well known (Wang *et al.* 1984). As an illustration two different structures of the $\Sigma = 5$ (210) symmetrical tilt boundary, B and B′, are presented in figure 1 *a*, *b* respectively, and two different structures of the $\Sigma = 5$ (001) twist boundary, CSL and type I, in figure 2 *a*, *b* respectively. These structures were calculated using potentials for gold. The planar repeat cell of the $\Sigma = 5$ (210) tilt boundary is delineated by the vectors [001] and [$\bar{1}$20] and the planar repeat cell of the $\Sigma = 5$ twist boundary by the vectors $\frac{1}{2}$[130] and $\frac{1}{2}$[3$\bar{1}$0]. In the following we shall call the unit cell of the boundary the parallelepiped based on the planar repeat cell extending away from the boundary into both the lower and upper grains.

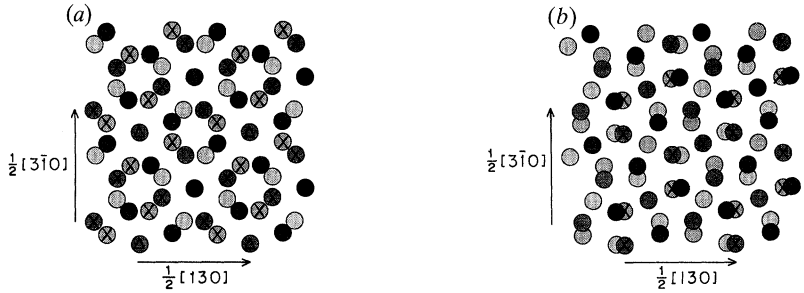

Figure 2. The relaxed structures of the $\Sigma = 5$ (001) twist boundaries calculated using the many-body potential for gold. (*a*) CSL structures, (*b*) type I structure. The atoms projected in the [001] direction, are depicted as shaded circles and four different shades represent atoms from four different (002) planes, two from the lower and two from the upper grain.

The boundary structures shown in figures 1 and 2 were calculated using potentials for gold but very similar structures, indistinguishable on the scale of the figures, were obtained using the potentials for copper. In the case of gold the structure B of the $\Sigma = 5$ (210) tilt boundary is a lower energy structure; the energy of the structure B′ is 15% higher. However, in the case of copper the situation is reversed. The energy of the structure B′ is 8% lower than the energy of the structure B. Furthermore, when introducing a small perturbation the structure B′ in gold readily transforms into B and in copper B transforms into B′. This suggests that structure B′ in gold and B in copper are unstable which is corroborated by the analysis of the elastic moduli presented in §5.

The structures of the $\Sigma = 5$ twist boundary shown here are only two possibilities of a number of other structures found in previous studies (Bristowe & Crocker 1978; Oh & Vitek 1986). The CSL structure (figure 2*a*) possesses the symmetry corresponding to the space group $p42_1'2'$ (Pond & Bollmann 1979). The primes on the two-fold axes indicate that the symmetry elements relate sites in different crystals. The four fold axis is parallel to [001], and the $2_1'$ and $2'$ axes lie in the interface halfway between the nearest (002) planes of both crystals and relate atoms in the two grains (Schwartz *et al.* 1985). The space group of the Type I structure (figure 2*b*) is $p22_1'2'$, and thus it has a lower symmetry. Nevertheless, the Type I structure is a lower energy structure as noted in a number of previous calculations (Bristowe & Crocker 1978; Schwartz *et al.* 1985, 1988; Oh & Vitek 1986). However, the energy difference between these two structures is in the case of gold only 4%.

3. Elastic moduli of heterogeneous continua

In this section we briefly discuss various continuum mechanics concepts that apply both to the interpretation of the elastic constants of the discrete, atomically heterogeneous systems that are introduced in §4 and to the corresponding continuum model which is introduced in §5. Conditions of positive definiteness and strong ellipticity of elastic moduli are defined and their implications are discussed. Notions of averages and effective properties (i.e. overall or macroscopic properties) for heterogeneous continua are also introduced. Finally, both upper and lower bounds on the elastic moduli are given with special attention paid to restrictions imposed by the elasticities.

PHILOSOPHICAL TRANSACTIONS OF THE ROYAL SOCIETY A MATHEMATICAL, PHYSICAL & ENGINEERING SCIENCES

(a) Strain measure and definition of elastic moduli

The elastic constants of a continuum or a system of particles can be rigorously defined through considerations of the change in energy with respect to straining of these systems. The precise values of these elastic constants, e.g. moduli, depend upon the strain measure adopted and, therefore, we begin by discussing kinematics of deformation and introduce a particular strain measure. It is well known that there are an infinity of strain measures that characterize the deformation or straining of material line segments (Hill, 1968, 1978; Mehrabadi & Nemat-Nasser 1987), although in practice only a few are commonly used. Here we choose the lagrangian strain (sometimes referred to as the Green strain). For this definition of strain, the effective elastic moduli of discrete atomic structures have all the symmetry properties normally associated with rotational invariance, as shown by Martin (1975*b*).

Let the vectors $\boldsymbol{X}$ and $\boldsymbol{x}$ denote material points in an undeformed and deformed configuration, respectively, where for continuum deformation one can regard $\boldsymbol{x}$ as a continuous function of $\boldsymbol{X}, \boldsymbol{x}(\boldsymbol{X})$. In terms of cartesian components the deformation gradient is then defined as

$$F_{ij} = \partial x_i / \partial X_j \tag{3.1}$$

and the components of the lagrangian strain as

$$\epsilon_{ij} = \tfrac{1}{2}(F_{ki} F_{kj} - \delta_{ij}), \tag{3.2}$$

where δ_{ij} is the Kronecker delta. In terms of the displacement vector u_i, where $x_i = X_i + u_i$, the components of ϵ_{ij} can also be expressed as

$$\epsilon_{ij} = \frac{1}{2}\left(\frac{\partial u_i}{\partial X_j} + \frac{\partial u_j}{\partial X_i} + \frac{\partial u_k}{\partial X_i}\frac{\partial u_k}{\partial X_j}\right). \tag{3.3}$$

If the displacement gradients are small so that the quadratic terms in (3.3) are negligible, ϵ_{ij} is just the symmetric part of the displacement gradient which is the usual small strain definition adopted in the linear theory of elasticity. In uniaxial deformation, for example, with $x_1 = \lambda X_1, \epsilon_{11} = \frac{1}{2}(\lambda^2 - 1)$. For an affine transformation $u_i = u_i^0 + A_{ij} x_j$ the displacement gradients are $\partial u_i / \partial X_j = A_{ij}$, where u_i^0 and A_{ij} are constant tensors. Analyses of the continuum model discussed in §§3*b* and 3*d* are based on small-strain elasticity, $O(\epsilon_{ij}) \ll 1$.

For an arbitrary uniform strain, ϵ_{ij}, the change in the strain energy, U, of a body of volume Ω can be formally expressed as a Taylor series

$$\Delta U = \Omega[\sigma_{ij}\epsilon_{ij} + \tfrac{1}{2}C_{ijkl}\epsilon_{ij}\epsilon_{kl} + O(\epsilon^3)], \tag{3.4}$$

where

$$\sigma_{ij} = \frac{1}{\Omega}\left(\frac{\partial U}{\partial \epsilon_{ij}}\right)_{\epsilon_{ij}=0} \tag{3.5a}$$

is the tensor of the first-order elastic constants or internal stresses and

$$C_{ijkl} = \frac{1}{\Omega}\left(\frac{\partial^2 U}{\partial \epsilon_{ij}\partial \epsilon_{kl}}\right)_{\epsilon_{ij}=0} \tag{3.5b}$$

is the tensor of the second-order elastic constants or elastic moduli of the medium. The exact values of these constants depend on the strain measure used and, as noted above, we adopt here the lagrangian strain measure.

(*b*) *Properties of elastic moduli*

The fourth-order tensor of elastic moduli $\boldsymbol{C}$ is said to be *positive definite* if for any non-zero second-order, symmetric tensor $\boldsymbol{\varepsilon}$

$$C_{ijkl}\,\epsilon_{ij}\,\epsilon_{kl} > 0, \quad \epsilon_{ij} \neq 0. \tag{3.6}$$

With the usual symmetries, i.e. $C_{ijkl} = C_{jikl} = C_{klij}$, $\boldsymbol{C}$ can be represented in the usual way by a 6×6 symmetric matrix. Then, positive definiteness requires that all six eigenvalues of this matrix be positive (or non-negative for positive semi-definite), and this condition can be readily checked for each phase. If (3.6) is satisfied then the strain energy is always positive at every strained point in a deformed body. It may be of interest to note that in the isotropic case, positive definiteness of $\boldsymbol{C}$ requires that the shear modulus $G > 0$ and $-1 < \nu < \frac{1}{2}$, where ν is the Poisson's ratio, in which case the bulk modulus $K > 0$ and the Young's modulus $E > 0$. If $\boldsymbol{C}$ is positive semi-definite, i.e. the symbol $>$ in (3.6) is replaced by $\geqslant$, then $G \geqslant 0$ and $-1 \leqslant \nu < \frac{1}{2}$.

The differential equations of equilibrium of a linear elastic continuum, expressed in terms of the displacements (the Navier equations) are *strongly elliptic* if for any two non-zero vectors ξ_i and η_i

$$C_{ijkl}\,\xi_i\,\xi_k\,\eta_j\,\eta_l > 0, \quad \xi_i \neq 0 \quad \text{and} \quad \eta_i \neq 0. \tag{3.7}$$

If (3.7) is satisfied then waves travel with real, positive velocities through the elastic solid and, at least in the case when the average strain is zero, the total strain energy of any deformed body is non-negative (see Knops & Payne 1971). If the average strain $\bar{\epsilon}_{ij}$ (see equation (3.8) below) is non-zero then the total strain energy is at least greater than or equal to $C_{ijkl}\,\bar{\epsilon}_{ij}\,\bar{\epsilon}_{kl}$, where for some $\bar{\epsilon}_{ij}$ the latter may be negative if the moduli are not positive definite. When the Navier equations are no longer elliptic, displacement-gradient discontinuities, for example in the form of shear bands, become admissible.

Unlike the condition for positive definiteness, the weaker condition of strong ellipticity is not easily checked. To see this we note that (3.7) implies that the 3×3 matrix $C_{ijkl}\,\xi_i\,\xi_k$ must be positive definite for any ξ_i (for which there are an infinity of cases to check). In the isotropic case, strong ellipticity requires that the shear modulus $G > 0$ and $-\infty < \nu < \frac{1}{2}$ or $1 < \nu < +\infty$, in which case the bulk and Young's moduli could be positive or negative. If $\boldsymbol{C}$ is semi-strongly elliptic, i.e. the symbol $>$ in (3.7) is replaced by $\geqslant$, then $G \geqslant 0$ and ν lies in the same range.

The notion of positive definite and strongly elliptic moduli will be used to interpret the discrete (atomistically) defined moduli. It is found that for certain atoms the moduli are not positive definite and for some not even strongly elliptic. Certain other important consequences of positive definiteness (3.6) and strong ellipticity (3.7) relate to the determination of bounds on the effective moduli. First, if the moduli of each phase of a heterogeneous medium are positive definite, i.e. (3.6) is satisfied for each phase, and displacements are continuous across interfaces (i.e. perfect bonding), then the actual internal fields for any proper boundary-value problem (BVP) are unique and minimize both potential energy and complementary energy. (For a proper BVP, $\boldsymbol{u}$ or $\boldsymbol{T}$ or some linear combination of the two are prescribed on each point of the external boundary S_Ω, where $\boldsymbol{u}$ is the displacement vector, $\boldsymbol{T}$ is the traction vector.) If the moduli of each phase are positive semi-definite then the solution may not be unique for every proper BVP but a minimum in potential energy exists. Second, if the strongly elliptic condition (3.7) is satisfied for a homogeneous medium,

then the actual internal fields for *prescribed displacements* on the boundary are also unique and minimize the potential energy (see, for example, Gurtin 1963). If the moduli are semi-strongly elliptic then for every displacement BVP the solution may not be unique but a minimum exists. (The reader is referred to Knops & Payne (1971) for an expanded discussion of uniqueness.) The existence of these minima make it possible to determine bounds on the effective moduli. Without positive definiteness, a complementary energy principle is generally not valid.

(c) *Effective moduli of a heterogeneous continuum*

Let us consider a heterogeneous continuum composed of homogeneous phases with volumes Ω^α and elastic moduli C^α_{ijkl}; here α denotes different phases. When such a medium is loaded on the external boundary by either a uniform traction or a displacement corresponding to a uniform strain then, in general, the stresses and strains in the interior will be non-uniform. A fundamental problem of interest which has been widely studied in the continuum mechanics is the determination of overall or effective response of the heterogeneous medium (see, for example, Hashin 1983; Willis 1981, 1983; Hill 1985; Walpole 1983; Milton & Kohn 1988). For the problem of external loading by either a uniform traction or strain field, these effective properties, i.e. effective elastic moduli, relate average stresses and average strains as detailed below.

Formally, $\bar{\sigma}_{ij}$ and $\bar{\epsilon}_{ij}$ are defined to be the volume averages of local stresses σ_{ij} and strains ϵ_{ij} respectively, in the heterogeneous medium:

$$\bar{\sigma}_{ij} \equiv \frac{1}{\Omega}\int \sigma_{ij}\,\mathrm{d}\Omega, \quad \bar{\epsilon}_{ij} \equiv \frac{1}{\Omega}\int \epsilon_{ij}\,\mathrm{d}\Omega. \tag{3.8}$$

If the local stresses are an equilibrium field which, in the absence of body forces, are divergence free ($\sigma_{ij,j} = 0$), and the strains are small (infinitesimal) and, therefore, equal to the symmetric part of the displacement gradient (equation (3.3)), then these averages are connected to uniform boundary conditions in the following way. Let S_Ω denote the boundary of Ω and let $\boldsymbol{n}$ be the unit outward normal to S_Ω. First, if the uniform traction vector $T_i = \sigma^0_{ij} n_j$ is applied to S_Ω, where σ^0_{ij} is constant, then application of the divergence theorem to (3.8) gives $\bar{\sigma}_{ij} = \sigma^0_{ij}$. Second, if the displacement field $u_i = \epsilon^0_{ij} x_j$, corresponding to the uniform and constant strain ϵ^0_{ij} is applied on S_Ω then $\bar{\epsilon}_{ij} = \epsilon^0_{ij}$. Furthermore, for either of these fields, using (3.8),

$$\bar{\sigma}_{ij}\,\bar{\epsilon}_{ij} = \frac{1}{\Omega}\int \sigma_{ij}\,\epsilon_{ij}\,\mathrm{d}\Omega. \tag{3.9}$$

Now, the overall effective moduli, C^*_{ijkl}, for the heterogeneous medium are defined by the relation

$$\bar{\sigma}_{ij} = C^*_{ijkl}\,\bar{\epsilon}_{kl}. \tag{3.10}$$

The effective moduli are designated by an asterisk rather than an overbar to emphasize that they are not simply volume averages of the moduli of individual phases. Even in the framework of linear elasticity, if we imagine a well-defined heterogeneous medium in terms of geometry and phase properties, the exact calculation of C^*_{ijkl} is a formidable if not impossible task since partial differential equations must be solved for a heterogeneous medium that possesses a rather irregular phase geometry. Instead, the approach most often taken is to approximate

the effective continuum properties in terms of bounds on the moduli which are rigorous bounds only if all of the C^{α}_{ijkl} satisfy certain restrictions that are classified in the previous section. On the other hand, the exact values of C^{*}_{ijkl} can be calculated for the systems composed of discrete particles, as described in §4.

(*d*) *Bounds on effective moduli*

Consider a heterogeneous continuum (which is piecewise continuous) and let $\boldsymbol{C}^{\alpha}$ denote the moduli for phase α. When certain restrictions on the phase moduli $\boldsymbol{C}^{\alpha}$ are satisfied, then rigorous bounds on the effective moduli $\boldsymbol{C}^{*}$ can be obtained corresponding to prescribed uniform straining on the boundary of the heterogeneous medium. For the atomically heterogeneous systems under investigation, due to the general anisotropy and possible loss of positive definiteness for the moduli of individual phases, particularly those at the interface, we first focus on the application and generalization of the simplest of the classical bounds. (Even though the grain boundaries under consideration contain internal stresses, so long as these are divergence free, as are residual stresses in a continuum, they will not change the structure of the classical bounds.) The simplest case is when the $\boldsymbol{C}^{\alpha}$s are positive definite as defined in (3.6) for each phase. In this case, the principle of minimum potential energy leads to the Voigt upper bound which is associated with uniform strain throughout the heterogeneous medium equal to the prescribed or average strain (see, for example, Willis 1981)

$$\boldsymbol{C}_{\mathrm{V}} = \frac{1}{\Omega}\sum_{\alpha} \Omega^{\alpha}\boldsymbol{C}^{\alpha} \equiv \bar{\boldsymbol{C}}, \tag{3.11}$$

i.e. Voigt bound is simply the volume average, $\bar{\boldsymbol{C}}$, of the moduli of individual phases, the arithmetic mean. In the case of the Voigt bound, as well as the other bounds given below, only volume fraction, Ω_{α}/Ω, of individual phases and not, for example, absolute or relative positions of phases enter the expressions. These volume fractions in the present examples are directly determined from the volume of a Voronoi polyhedron associated with a particular atom.

Also, in the case of positive definite moduli, the principle of minimum complementary energy leads to the Reuss lower bound which is associated with uniform stressing throughout the heterogeneous medium equal to the average stress

$$\boldsymbol{C}_{\mathrm{R}} = \left[\frac{1}{\Omega}\sum_{\alpha} \Omega^{\alpha}(\boldsymbol{C}^{\alpha})^{-1}\right]^{-1}, \tag{3.12}$$

i.e. the Reuss bound is simply the inverse of the volume average of inverses, the harmonic mean. The fact that this lower bound does not permit semi-definiteness or some cases of indefiniteness of the phase moduli, i.e. one or more eigenvalues of the moduli are zero, is readily seen since (3.12) involves inverses of these moduli. Finally, it is important to note that the expressions in (3.11) and (3.12) are bounds in the sense that the associated quadratic forms are bounded, i.e. for any $\bar{\boldsymbol{\varepsilon}}$

$$\bar{\boldsymbol{\varepsilon}}\boldsymbol{C}_{\mathrm{R}}\bar{\boldsymbol{\varepsilon}} \leqslant \bar{\boldsymbol{\varepsilon}}\boldsymbol{C}^{*}\bar{\boldsymbol{\varepsilon}} \leqslant \bar{\boldsymbol{\varepsilon}}\boldsymbol{C}_{\mathrm{V}}\bar{\boldsymbol{\varepsilon}}, \tag{3.13}$$

where the fourth-order product $\bar{\boldsymbol{\varepsilon}}\boldsymbol{C}\bar{\boldsymbol{\varepsilon}} = C_{ijkl}\,\epsilon_{ij}\,\epsilon_{kl}$. Therefore, from (3.13) we can most readily obtain explicit bounds on the diagonal components of $\boldsymbol{C}^{*}$.

Next, we consider the possibility when the moduli of one or more of the individual phases are not positive definite. In this case we assume that all phases are at least

strongly elliptic as defined in (3.7) (or semi-strongly elliptic, but here the distinction is not significant). In this case, for displacement BVPs for which the principle of minimum potential energy still holds, the Voigt upper bound (3.11) is still valid. Gurtin (1963) has established this principle in the case of homogeneous solids; Professor J. R. Willis of Bath University, U.K. has established this principle for heterogeneous solids when a null-lagrangian (or variationally trivial lagrangian) Λ_{ijkl} can be found such that $C_{ijkl}+\Lambda_{ijkl}$ is positive definite for each phase. On the other hand, the Reuss lower bound is not valid (i.e. the principle of minimum complementary energy no longer exists and inverses in (3.12) may not exist). This poses a difficult problem for which there may be solutions but, nevertheless, the moduli of individual phases may be so poorly conditioned that it is impossible to construct rigorous bounds.

We will now consider an extension of the translation method that has been developed recently by Francfort & Murat (1986) and Milton (1990) to construct a lower bound on $\boldsymbol{C}^*$ when one or more of the phases is not positive definite. The extension we have made permits the phase moduli to be strongly elliptic rather than positive definite as they assume. Since the former also leads to the principle of minimum potential energy for displacement BVPs, the extension is straightforward. A derivation of the lower bound based upon the translation method is given in Appendix A. Let $\boldsymbol{C}^0$ be a constant fourth-order tensor that translates the local moduli in a heterogeneous medium such that $\boldsymbol{C}^\alpha-\boldsymbol{C}^0$ is a positive definite (or positive semi-definite) for each phase, and, most importantly in the present application, that the quadratic form $\boldsymbol{\varepsilon}\boldsymbol{C}^0\boldsymbol{\varepsilon}$ is quasi-convex with respect to all symmetric second-order tensors $\boldsymbol{\varepsilon}$. With these conditions on the $\boldsymbol{C}^\alpha$s and $\boldsymbol{C}^0$, from the principles of minimum complementary energy and minimum potential energy for the translated material it can be shown that (see Milton (1990) in the case where all phases are positive definite and Appendix A when only strong ellipticity is required)

$$\bar{\boldsymbol{\varepsilon}}\left\{\left[\frac{1}{\Omega}\sum_\alpha \Omega^\alpha(\boldsymbol{C}^\alpha-\boldsymbol{C}^0)^{-1}\right]^{-1}+\boldsymbol{C}^0\right\}\bar{\boldsymbol{\varepsilon}}\leqslant\bar{\boldsymbol{\varepsilon}}\boldsymbol{C}^*\bar{\boldsymbol{\varepsilon}}. \tag{3.14}$$

This expression leads to a lower bound, $\boldsymbol{C}_{\mathrm{T}}$, on the effective moduli $\boldsymbol{C}^*$ based upon a translation of the effective elastic constants:

$$\boldsymbol{C}_{\mathrm{T}}=\left[\frac{1}{\Omega}\sum_\alpha \Omega^\alpha(\boldsymbol{C}^\alpha-\boldsymbol{C}^0)^{-1}\right]^{-1}+\boldsymbol{C}^0. \tag{3.15}$$

If the individual phases are not translated, i.e. $\boldsymbol{C}^0=\boldsymbol{0}$, then $\boldsymbol{C}_{\mathrm{T}}=\boldsymbol{C}_{\mathrm{R}}$. Hence, when all phases are at least strongly elliptic then

$$\bar{\boldsymbol{\varepsilon}}\boldsymbol{C}_{\mathrm{T}}\bar{\boldsymbol{\varepsilon}}\leqslant\bar{\boldsymbol{\varepsilon}}\boldsymbol{C}^*\bar{\boldsymbol{\varepsilon}}\leqslant\bar{\boldsymbol{\varepsilon}}\boldsymbol{C}_{\mathrm{V}}\bar{\boldsymbol{\varepsilon}}. \tag{3.16}$$

Finally, we emphasize that if the associated restrictions (see §3*b* and Appendix A) are met, then (3.11), (3.12) and (3.15) are rigorous bounds on the effective moduli $\boldsymbol{C}^*$ for a heterogeneous continuum. As we shall see, it turns out that certain phases near the grain boundary (whose properties are determined from the atomistic simulation) violate these restrictions so that $\boldsymbol{C}_{\mathrm{V}}$, $\boldsymbol{C}_{\mathrm{R}}$ and $\boldsymbol{C}_{\mathrm{T}}$ are not rigorous bounds. For example, if some $\boldsymbol{C}^\alpha$ is not strongly elliptic then certainly $\boldsymbol{C}_{\mathrm{V}}$ is not a rigorous upper bound and, in general, a quasi-convex $\boldsymbol{C}^0$ cannot be found, so that $\boldsymbol{C}_{\mathrm{T}}$ is not a rigorous lower bound. Nevertheless, we will regard these as estimates and see that in most cases they do behave as bounds.

4. Atomic level and effective elastic moduli for periodic discrete structures

To evaluate the elastic moduli for a discrete medium in which the atomic interactions are known we shall consider a three-dimensionally periodic structure with the repeat cell containing N non-equivalent atoms, i.e. those which are not related by any symmetry operation of the structure. The volume of this cell is equal to Ω. We assume further that the total energy of the system, U, can be written as

$$U = \sum_{\alpha} U_{\alpha}, \tag{4.1}$$

where the summation extends over all the atoms. U_{α} is the energy associated with the atom α and it is a function of the vectors, $\boldsymbol{R}^{\alpha\beta}$, separating atom α and other atoms β. It was recognized long ago (see, for example, Born & Huang 1954) that when a macroscopically uniform strain is applied to this structure the displacements of different non-equivalent atoms are generally different, i.e. an internal relaxation occurs. This is analogous to the situation that arises in the continuum mechanics of heterogeneous media subject to uniform external loading, discussed in the preceding section. In both cases such internal relaxations have to be taken into account when evaluating the effective elastic moduli defined by equation (3.10).

However, unlike the situation for a continuum, exact values of effective elastic moduli may be calculated for the system of discrete particles for which the energy of the system, U, is a known function of the positions of the particles. This problem was solved using the method of long waves by Born & Huang (1954) and Maradudin *et al.* (1971), while Martin (1975*b*) treated this problem for general many-body atomic interactions employing the method of uniform macroscopic deformations. One very important aspect of the results presented in this paper is that the complete fourth-order elastic modulus tensor is calculated for both the local and the effective properties. Below, the principal results of Martin (1975*b*) are summarized.

When applying a macroscopically uniform strain $\bar{\epsilon}_{ij}$ the displacements of atoms in the repeat cell can be divided into the 'homogeneous' ones, which are linearly related to $\bar{\epsilon}_{ij}$ and the 'inhomogeneous' displacements resulting from the internal relaxation. If no internal relaxation takes place the change in total energy is given by (3.4) with all quantities in square brackets replaced by their averages. The average of the first-order elastic constants, i.e. the internal stresses, are then

$$\begin{aligned}\bar{\sigma}_{ij} &= \frac{1}{\Omega}\frac{\partial U}{\partial \epsilon_{ij}} = \frac{1}{\Omega}\sum_{\alpha=1}^{N}\sum_{\beta}\frac{\partial U_{\alpha}}{\partial R_i^{\alpha\beta}}R_j^{\alpha\beta} \\ &\equiv \frac{1}{\Omega}\sum_{\alpha=1}^{N}\Omega^{\alpha}\sigma_{ij}^{\alpha},\end{aligned} \tag{4.2}$$

and the average of the moduli

$$\begin{aligned}\bar{C}_{ijkl} &= \frac{1}{\Omega}\frac{\partial^2 U}{\partial \epsilon_{ij}\partial \epsilon_{kl}} = \frac{1}{\Omega}\sum_{\alpha=1}^{N}\sum_{\beta}\frac{\partial^2 U_{\alpha}}{\partial R_i^{\alpha\beta}\partial R_k^{\alpha\beta}}R_j^{\alpha\beta}R_l^{\alpha\beta} \\ &\equiv \frac{1}{\Omega}\sum_{\alpha=1}^{N}\Omega^{\alpha}C_{ijkl}^{\alpha},\end{aligned} \tag{4.3}$$

where the sum on β includes all interacting neighbours of atom α (including those

from other periodic cells) and the derivatives are evaluated at zero strain and Ω^α is the volume associated with the atom α, which can be identified with the volume of the corresponding Voronoi polyhedron ($\Omega = \sum_{\alpha=1}^{N} \Omega^\alpha$). This is the case when all the atoms in the repeat cell are equivalent as, for example, in centrosymmetric structures. The algebraic equalities (4.2) and (4.3) through the summations over α then formally define the atomic level stresses σ_{ij}^α and atomic level moduli C_{ijkl}^α respectively. The derivatives in (4.2) and (4.3) are readily evaluated from (4.1) with given particular forms for V and Φ in (2.1) and corresponding formulae are given in Appendix B.

When the repeat cell of the particle system contains non-equivalent atoms relaxation occurs and the corresponding inhomogeneous atomic displacements are determined by the auxiliary condition of zero forces on each atom of the strained medium. It was shown by Martin (1975*b*) that internal stresses are not affected by the relaxation and are still given by equation (4.2). However, the relaxation alters the elastic moduli. The change in total energy is now given by an expression analogous to (3.4) with σ_{ij} and ϵ_{ij} replaced by their averages $\bar{\sigma}_{ij}$ and $\bar{\epsilon}_{ij}$, while C_{ijkl} is replaced by the effective elastic moduli

$$C_{ijkl}^* = \bar{C}_{ijkl} + \tilde{C}_{ijkl}, \tag{4.4}$$

where $\bar{C}_{ijkl}$, defined in (4.3), is the volume average of the C_{ijkl}^α, and the second term is the relaxation part of the moduli. This part can be evaluated analytically as follows (Martin 1975*b*):

$$\tilde{C}_{ijkl} = -\frac{1}{\Omega} \sum_{\alpha=2}^{N} \sum_{\beta} D_{ijn}^\alpha g_{nm}^{\alpha\beta} D_{mkl}^\beta, \tag{4.5}$$

where

$$D_{ijn}^\alpha = \frac{\partial^2 U}{\partial \epsilon_{ij} \partial R_n^{\alpha 1}} \tag{4.6a}$$

and $g_{nm}^{\alpha\beta}$ is the inverse of the matrix

$$E_{pq}^{\alpha\beta} = \frac{\partial^2 U}{\partial R_p^{\alpha 1} \partial R_q^{\beta 1}}, \tag{4.6b}$$

so that

$$\sum_{\beta} g_{nm}^{\alpha\beta} E_{mq}^{\beta\gamma} = \delta_{nq} \delta_{\alpha\gamma}, \tag{4.6c}$$

where the origin of the repeat cell is identified with the atom number 1. Detailed expressions for σ_{ij}^α, C_{ijkl}^α, D_{ijn}^α and $E_{pq}^{\alpha\beta}$, when the energy per atom is given by equation (2.1), are presented in Appendix B.

Just as the homogeneous elastic moduli for each atom α, can be formally defined from equation (4.3), the relaxation part of the moduli can also be associated with individual atoms since according to equation (4.5)

$$\tilde{C}_{ijkl} = \frac{1}{\Omega} \sum_{\alpha=2}^{N} \Omega^\alpha \tilde{C}_{ijkl}^\alpha, \tag{4.7a}$$

where

$$\tilde{C}_{ijkl}^\alpha = -\frac{1}{\Omega^\alpha} \sum_{\beta} D_{ijn}^\alpha g_{nm}^{\alpha\beta} D_{mkl}^\beta. \tag{4.7b}$$

PHILOSOPHICAL TRANSACTIONS OF THE ROYAL SOCIETY A MATHEMATICAL, PHYSICAL & ENGINEERING SCIENCES

It is seen from equations (3.4) and (4.1) to (4.7) that the change in energy, per unit volume, associated with an infinitesimal uniform strain $\bar{\epsilon}_{ij}$ can be formally expressed via the atomic level stresses and moduli as

$$\Delta U = \frac{1}{\Omega} \sum_{\alpha=1}^{N} \Omega^{\alpha} [\sigma_{ij}^{\alpha} \bar{\epsilon}_{ij} + \tfrac{1}{2} C_{ijkl}^{*\alpha} \bar{\epsilon}_{ij} \bar{\epsilon}_{kl} + O(\bar{\epsilon}^3)]. \tag{4.8}$$

In the next section, based upon the formulae given in this section, the moduli for individual atoms in various periodic structures containing grain boundaries are calculated. Then the exact effective moduli for the overall structures are calculated and compared with bounds on the effective moduli for an associated heterogeneous continuum.

5. Grain boundaries as heterogeneous continua on the atomic scale

The definition of atomic level stresses and elastic moduli introduced above naturally leads to a model of a heterogeneous continuum in which individual phases are identified with individual atoms. Each phase is geometrically constructed as the Voronoi polyhedron associated with an individual atom. As a schematic illustration, the construction of Voronoi polyhedra is depicted in figure 3 for the unrelaxed $\Sigma = 5$ (210) tilt boundary in a simple cubic lattice. In this case the Voronoi polyhedra in the ideal crystal (Wigner–Seitz cells) are cubes and their projections onto the (001) plane are squares while for the FCC lattice the Voronoi polyhedra are rhombic dodecahedra (Kittel 1986) and the projection would be complex. The moduli of each phase are identified with the corresponding atomic level moduli C_{ijkl}^{α}, determined by equation (4.3). Such a construction is, of course, meaningful only if it leads to a model of a heterogeneous continuum whose overall properties closely approximate the properties of the actual discrete system. Typically, when this agreement between the discrete and continuum effective properties is found, the structure possesses a minimum energy among all known structures and is termed stable. More specifically, as seen below, this agreement is in the sense that the exact effective moduli lie between the upper and lower bounds (estimates) for the continuum model. In cases where structures of a particular boundary have exact effective moduli that lie below the lower bound (estimate), local stability of these structures seems to be common. Nevertheless, these structures are usually higher energy structures and we regard them, therefore, as 'metastable' in the sense that they may be stable for small perturbations, but are unstable for large perturbations. On the other hand, when the exact effective moduli lie above the upper bound the structure is typically not even locally stable, i.e. it is unstable. The B′ structure in gold and the B structure in copper are examples of unstable structures.

Since both the discrete and the piecewise continuous media are heterogeneous, each will undergo a *non-uniform* internal response to a *uniform* external loading. The corresponding effective moduli of the discrete structure can be computed exactly (§4 and Appendix B) while generally only upper and lower bounds on the effective moduli can be found for the continuum model (§3*d*). Comparison of the moduli calculated exactly for the discrete structure and the continuum bounds then reveals how closely the continuum analogue approximates the atomic model. This comparison is the main topic of this section and the principal result of this paper. Conversely, the continuum ideas introduced in §3 also aid in the interpretation of the

PHILOSOPHICAL TRANSACTIONS OF THE ROYAL SOCIETY A MATHEMATICAL, PHYSICAL & ENGINEERING SCIENCES

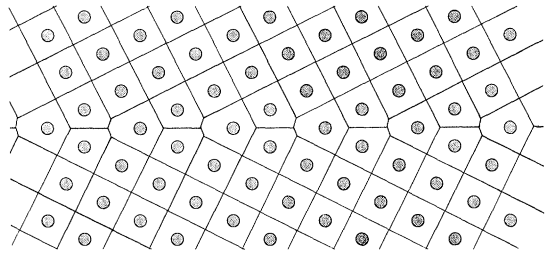

Figure 3. Schematic picture of Voronoi polyhedra associated with individual atoms in the $\Sigma = 5$ (210) tilt boundary in a simple cubic lattice.

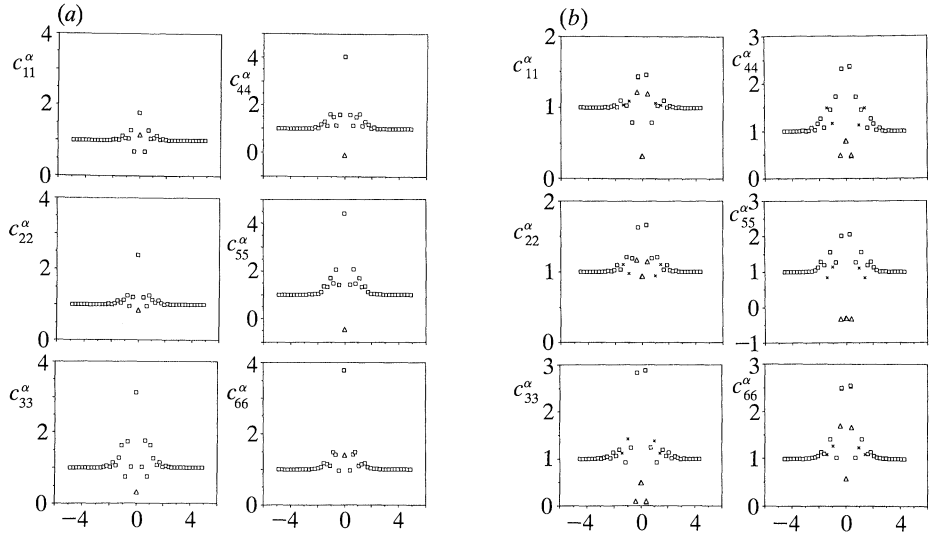

Figure 4. The normalized diagonal elements of the tensor of the atomic level moduli, $c^{\alpha}_{nn} = C^{\alpha}_{nn}/C^{0}_{nn}$, for the $\Sigma = 5$ [001]/(210) symmetrical tilt boundary in gold. (*a*) B structure, (*b*) B′ structure.

atomistic results, for example in cases where the moduli for an individual atom may not be positive definite or, in some cases, may not even be strongly elliptic. In the next section we first present the atomic level moduli calculated for the boundaries studied and discuss their characteristic features which for certain atoms in the interface may be rather unusual.

(*a*) *Atomic level moduli at grain boundaries*

The diagonal elements of the tensor of the atomic level moduli, C^{α}_{ijkl}, are displayed in figures 4 and 5 for the $\Sigma = 5$ (210) symmetrical tilt boundaries in gold and copper, respectively, and in figure 6 for the $\Sigma = 5$ [001] twist boundary in gold. The usual 6×6 matrix representation of the tensor of elastic constants is adopted and normalized values $c^{\alpha}_{nn} = C^{\alpha}_{nn}/C^{0}_{nn}$ (no summation over n), where C^{0}_{nn} is the corresponding modulus in the ideal lattice, are plotted; C_{11}, C_{22} and C_{33} are normal moduli while C_{44}, C_{55} and C_{66} are shear moduli. The C^{α}_{nn} and C^{0}_{nn} are defined in the natural interface coordinate system, specified in §2. For the boundaries studied here the elastic constants far away from the boundary are always the same for the lower and upper grain and possess the symmetry of the ideal lattice. The corresponding components of the moduli of the ideal lattice in the interface coordinate system are

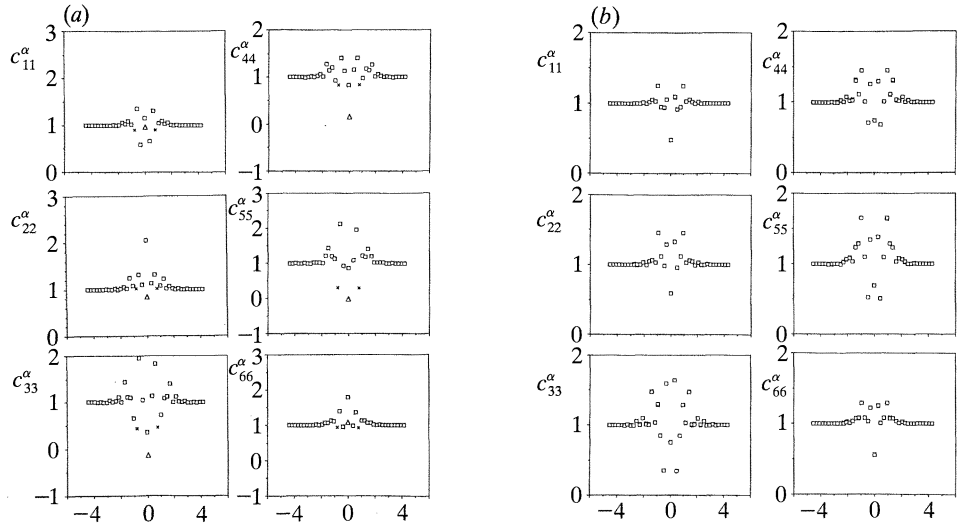

Figure 5. The normalized diagonal elements of the tensor of the atomic level moduli, $c^\alpha_{nn} = C^\alpha_{nn}/C^0_{nn}$, for the $\Sigma = 5$ [001]/(210) symmetrical tilt boundary in copper. (*a*) B structure, (*b*) B′ structure.

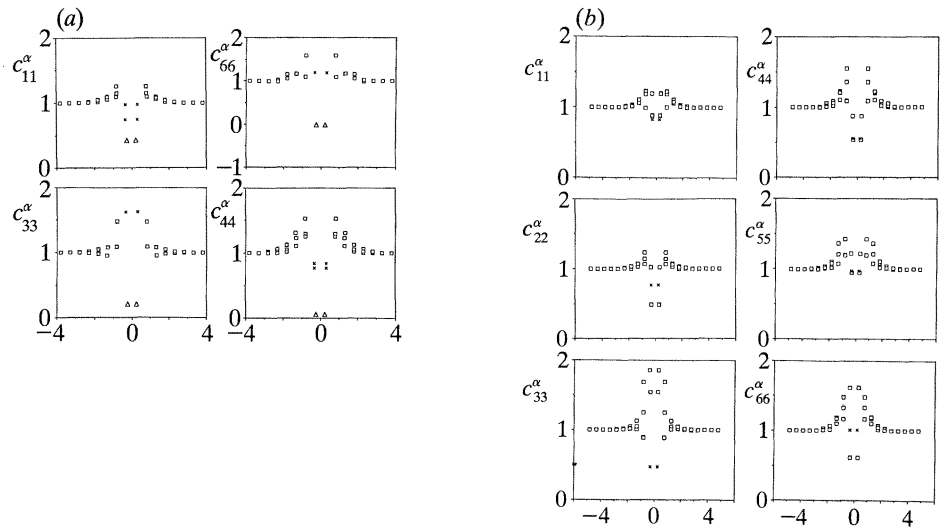

Figure 6. The normalized diagonal elements of the tensor of the atomic level moduli, $c^\alpha_{nn} = C^\alpha_{nn}/C^0_{nn}$, for the $\Sigma = 5$ [001] twist boundary in gold. (*a*) CSL structure, (*b*) type I structure.

listed in table 2 for each boundary considered. It is important to keep in mind that although the tensor of moduli for the ideal FCC lattice has only three distinct components, in the grain boundary region the moduli associated with individual atoms exhibit the general anisotropy and, therefore, the tensor of moduli has twenty-one distinct components. For brevity, only the six diagonal components are presented in this paper.

In figures 4–6 the points denote values of the moduli evaluated for individual atoms, where certain points correspond to more than one (equivalent) atom. The distances of particular atoms from the grain boundary are denoted on the horizontal

Table 2. *The diagonal components of the moduli (MPa) of the ideal lattice in the interface coordinate system for all the boundaries studied*

grain boundary	C_{11}	C_{22}	C_{33}	C_{44}	C_{55}	C_{66}
[001] tilt boundaries in gold						
$\Sigma 5$ (210) B	2.036	1.860	2.036	0.420	0.244	0.420
$\Sigma 5$ (210) B′	2.036	1.860	2.036	0.420	0.244	0.420
$\Sigma 5$ (310)	1.959	1.860	1.959	0.420	0.321	0.420
$\Sigma 13$ (320)	2.094	1.860	2.094	0.420	0.186	0.420
$\Sigma 13$ (510)	1.901	1.860	1.901	0.420	0.379	0.420
$\Sigma 73$ (830)	1.979	1.860	1.979	0.420	0.301	0.420
[001] tilt boundaries in copper						
$\Sigma 5$ (210) B	2.016	1.684	2.016	0.754	0.422	0.754
$\Sigma 5$ (210) B′	2.016	1.684	2.016	0.754	0.422	0.754
[001] twist boundaries in gold						
$\Sigma 5$ CSL	1.959	1.959	1.860	0.420	0.420	0.321
$\Sigma 5$ type I	1.959	1.959	1.860	0.420	0.420	0.321
$\Sigma 13$ CSL	1.901	1.901	1.860	0.420	0.420	0.379

axes of the plots; they are taken as positive for the upper and negative for the lower grain. The choice of the origin for measuring the distance from the boundary is, of course, somewhat arbitrary and in the present study it has been identified with the position of the plane separating the two grains in the geometrically constructed, unrelaxed, structure.

It is seen that the atomic level moduli have significantly different values in the boundary region than in the ideal crystal but converge to the ideal lattice values as the separation from the boundary increases. Not only do the values of individual components vary, but so do the principal axes of anisotropy (as characterized in a six-dimensional space) which will be reported in a subsequent paper. In most cases, marked by squares, the elastic moduli are positive definite. However, for a limited number of atoms in the boundary region the moduli are not positive definite and in some cases even strong ellipticity cannot be guaranteed. For the atoms for which the strong ellipticity cannot be established the values of the moduli are marked by triangles, while for those with strongly elliptic but not positive definite moduli they are marked by crosses. For the $\Sigma = 5$ (210) tilt and $\Sigma = 5$ [001] twist boundaries in gold the atoms for which the moduli have these unusual properties are similarly marked in figures 1 and 2. Again we emphasize that, for brevity, only the diagonal components of the moduli are plotted. In the boundary region there is generally no symmetry and variations in the off-diagonal components are also significant.

For the (210) B and B′ in gold structures the shear moduli C_{44} and C_{55}, which correspond to shearing on a plane parallel to the boundary (i.e. both have an x_3 component), are negative for certain atoms. Recall that moduli are non-positive definite if at least one eigenvalue of the matrix of elastic constants is negative (see §3*b*). A negative diagonal component of the tensor of moduli firmly indicates that the moduli are not strongly elliptic. In the case of the B structure in gold two (one non-equivalent) atoms per unit cell have non-positive definite moduli and these also have negative shear moduli (figure 4*a*). In the B′ structure in gold fourteen (seven non-equivalent) atoms have non-positive definite moduli of which six (three non-equivalent) have negative shear moduli (figure 4*b*). In the case of copper there are no

Table 3. *Boundary energies and characteristics of the atomic level and effective moduli for all the boundaries studied*

grain boundary	energy/(mJ m^{-2})	number of atoms with non-positive definite moduli	sums of all negative eigenvalues of moduli	number of atoms with negative diagonal moduli (non-strongly elliptic)	h_0 (in units of the lattice parameter)
[001] tilt boundaries in gold					
$\Sigma5$ (210) B	674	2	−0.29200	2	1.12
$\Sigma5$ (210) B′	773	14	−2.96316	6	2.24
$\Sigma5$ (310)	695	3	−0.39471	1	0.00
$\Sigma13$ (320)	634	8	−1.00400	4	0.00
$\Sigma13$ (510)	734	4	−1.30489	1	0.35
$\Sigma73$ (830)	723	18	−2.11313	6	0.60
[001] tilt boundaries in copper					
$\Sigma5$ (210) B	1124	6	−0.87570	2	2.24
$\Sigma5$ (210) B′	1041	0	0.00000	0	1.57
[001] twist boundaries in gold					
$\Sigma5$ CSL	726	10	−2.04948	2	4.00
$\Sigma5$ type I	697	4	−1.28410	0	3.00
$\Sigma13$ CSL	583	18	−4.87230	0	1.11
$\Sigma25$ CSL	—	40	−5.74145	0	0.00

atoms with non-positive definite moduli in the B′ structure (figure 5*b*) while in the B structure six (three non-equivalent) atoms have non-positive definite moduli of which two (one non-equivalent) have negative shear moduli (figure 5*a*). It is interesting to note that the B′ structure in gold and the B structure in copper are higher energy states and they were found to be unstable in the sense that a small perturbation of these structures leads to relaxation into lower energy structures B and B′ in gold and copper respectively.

In the $\Sigma = 5$ CSL twist boundary in gold ten (two non-equivalent) atoms per unit cell have non-positive definite moduli and two of these also have negative shear modulus C_{66} (figure 6*a*). On the other hand, for the lower energy Type I structure there are no atoms having negative atomic level shear moduli although four (one non-equivalent) atoms have non-positive definite moduli (figure 6*b*).

We have considered a significant number of other cases including $\Sigma = 13$ and $\Sigma = 25$ twist boundaries and $\Sigma = 13$ and 73 tilt boundaries. For brevity, the detailed results for moduli at individual atoms will not be presented here. Nevertheless, for some of these boundaries the effective bicrystal properties are discussed in the next section. In general, the number of atoms that lose positive definiteness or strong ellipticity are small relative to the total number of atoms that account for the distinct grain boundary structure. The numbers of atoms with non-positive definite moduli and negative diagonal components of the tensor of moduli are summarized for all the boundaries studied in table 3.

(*b*) *Effective moduli for bicrystals*

In this study we deal with blocks of atoms contained within infinite bicrystals with the periodic boundaries in the middle. As explained above, for each bicrystal a heterogeneous continuum is constructed as an analogue where each phase occupies

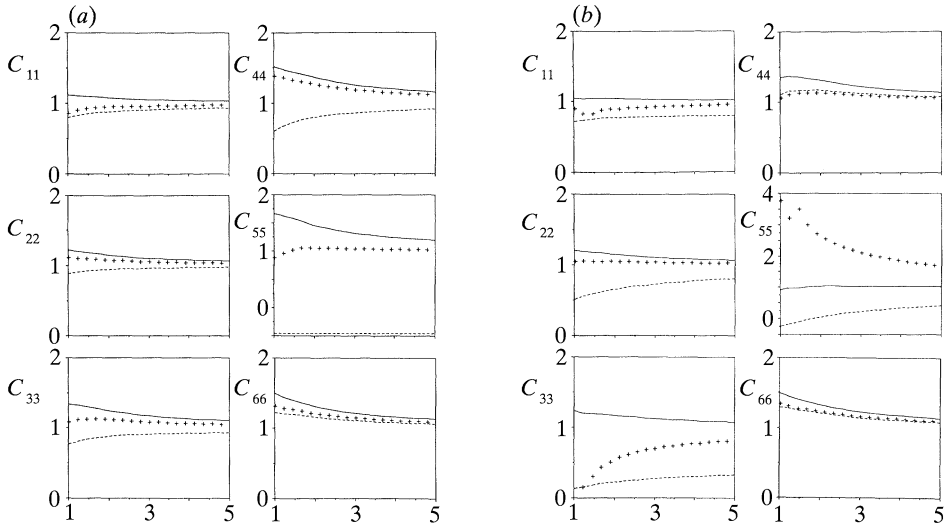

Figure 7. The effective moduli (points), the Voigt upper bound, $\boldsymbol{C}_{\mathrm{V}}$ (solid curve) and translation lower bound, $\boldsymbol{C}_{\mathrm{T}}$ (dashed curve) against the sub-block size h for the $\Sigma = 5$ [001]/(210) symmetrical tilt boundary in gold. (*a*) B structure, stable; (*b*) B′ structure, unstable.

the region in space defined by the Voronoi polyhedron for a particular atom and is assigned the elastic moduli for that atom. The exact effective moduli for the discrete atomistic system can be computed for the relaxed structure as described in §4. Now consider sub-blocks of the infinite bicrystal taken as small bicrystals in which the number of atom layers above and below the grain boundary is rather small. The height of these bicrystal sub-blocks is denoted $2h$. Since according to (4.7) contributions to the overall effective moduli can be associated with individual atoms, we may evaluate the exact effective moduli of each sub-block for the discrete model by summing $\boldsymbol{C}^{*\alpha}$ over the atoms in this sub-block. The effective moduli of the bicrystal are thus determined as functions of h.

Bounds on the effective moduli of the sub-blocks for the continuum model can be evaluated on the basis of the results in §3*d*. Summations in equations (3.11), (3.12) and (3.15) are always taken over the atoms in a sub-block and the bounds are thus also determined as functions of h. However, we must keep in mind that these are only rigorous bounds if each phase is at least strongly elliptic (and in the case of the translation lower bound, $\boldsymbol{C}_{\mathrm{T}}$, that the quadratic form associated with $\boldsymbol{C}^0$ is quasi-convex). Since most often at least one atom violates the strong ellipticity requirement, we regard $\boldsymbol{C}_{\mathrm{V}}$, $\boldsymbol{C}_{\mathrm{R}}$ or $\boldsymbol{C}_{\mathrm{T}}$ of §3*d* as estimates rather than bounds, although it is found that so long as $h > a$ (the lattice parameter) they tend to behave as bounds. For $\boldsymbol{C}_{\mathrm{T}}$ the translation operator $\boldsymbol{C}^0$ in (3.15) is taken to be a constant times the identity tensor for simplicity. (Other choices such as a constant times the ideal crystal moduli proved not to be more useful, probably because the anisotropy in the boundary region is quite general and not similar to that of the ideal crystal.)

In figures 7–13 the effective moduli $\boldsymbol{C}^*$ are plotted versus the sub-block size h. Each component plotted is normalized by the corresponding component for the ideal lattice, i.e. $C_{nn} = C^*_{nn}/C^0_{nn}$. The exact effective properties for the discrete (atomistic) system are denoted by points while the continuum estimates based on the Voigt upper bound, $\boldsymbol{C}_{\mathrm{V}}$, are the smooth curves and translation lower bound, $\boldsymbol{C}_{\mathrm{T}}$, are the dashed

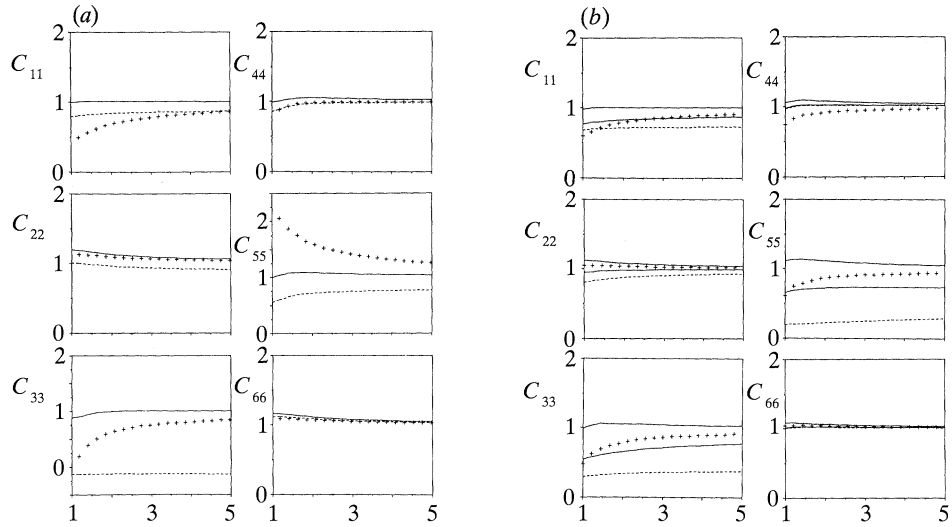

Figure 8. The effective moduli (points), the Voigt upper bound, $\boldsymbol{C}_{\mathrm{V}}$ (solid curve) and translation lower bound, $\boldsymbol{C}_{\mathrm{T}}$ (dashed curve) against the sub-block size h for the $\Sigma = 5$ [001]/(210) symmetrical tilt boundary in copper. (*a*) B structure, unstable; (*b*) B′ structure, stable. In the latter case the Reuss lower bound, $\boldsymbol{C}_{\mathrm{R}}$, is also drawn as a solid curve.

curves. In table 3 we give values of $h = h_0$ such that for $h < h_0$ the effective moduli for the discrete model are non-positive definite while for $h > h_0$ they are positive definite. Note that most often (and particularly for stable or metastable structures as defined below) h_0 is typically a small multiple of the lattice parameter. We begin with results for the $\Sigma = 5$ (210) symmetrical tilt boundary which are shown for gold and copper in figures 7 and 8 respectively.

For the B structure in gold (figure 7*a*) the exact effective moduli for the discrete structure always lie between the estimates as they should if the estimates are actual upper and lower bounds. The reason that the bounds (from here on the continuum estimates will be referred to as bounds) are not too close for certain shear components of the moduli is associated with corresponding components of the local moduli losing positive definiteness or strong ellipticity close to those directions. (In the case of loss of positive definiteness we mean those directions of eigenvectors corresponding to the negative eigenvalues in the six-dimensional hyperspace of the matrix of moduli while for the loss of ellipticity we simply mean that direction corresponding to a negative diagonal component of the moduli of any individual phase.) An extreme case for the B structure is the component C^*_{55} for which the lower bound is negative. For the structures B′ in gold (figure 7*b*) most of the effective moduli lie in between the bounds but C^*_{55} lies well above the upper bound which is physically implausible. From the continuum point of view the Voigt upper bound is based upon the assumption that each phase undergoes the same strain, equal to the average strain. This uniform strain mode of deformation is over constrained and, therefore, should lead to a stiffer effective response for the heterogeneous medium than the actual one. Similarly, from the point of view of the discrete structure the effective moduli, $\boldsymbol{C}^*$, are always smaller than the average moduli, $\bar{\boldsymbol{C}}$, which represent the Voigt upper bound. The reason is that they reflect the relaxation associated with application of the uniform strain and this always decreases the strain energy (see also equation (4.8)) provided the energy of the structure, considered as a function of coordinates of all the n atoms

in the block, is a minimum. Therefore, we suggest that the above situation may only arise if the structure is not stable. This means that the surface in the $3n$-dimensional space representing the dependence of the energy of the block on atomic positions does not possess a true local minimum for this configuration even though the forces acting on the atoms are all small, i.e. below the criterion used in the relaxation calculation (see §2). Such an energy surface is generally very complex and it may possess some plateaux and inflexions which may not be readily distinguishable from true minima.

First we note from table 3 that the energy of the B′ structure is in gold 15% higher than that for the B structure and, as mentioned in §2, the former readily transforms into the latter upon a small perturbation. Furthermore, as also seen in table 3, in the B structure the moduli of only *two* atoms per unit cell are not positive definite and these are also not strongly elliptic while for the B′ structure the moduli for *fourteen* atoms per unit cell are not positive definite and for six of these they are also not strongly elliptic. If the elastic moduli are not positive semi-definite, then upon deformation it is possible that the strain energy is negative at a material point, i.e. (3.6) may be violated locally. It means that local atom rearrangements arising from external loading (e.g. external displacements) can cause certain atoms to move to a locally lower energy configuration. This is entirely plausible even for stable structures since these correspond to local minima of the global energy and, while energy associated with some atoms decreases upon straining, it is compensated for by the increase of the energy associated with other atoms. However, it is unlikely that in stable structures such a decrease may occur for a large number of atoms. Hence, a large number of atoms with non-positive definite moduli is a good indication of possible instability of the structure. Indeed, at the plateau and/or inflexion of the energy surface defined above, the moduli which relate to the second derivatives of this surface, cannot be expected to be all positive definite. This is, presumably, the situation arising in the case of the B′ structure in gold.

The atomic configurations of the B and B′ structures in copper very closely resemble those of gold but the energy and moduli are quite different. As seen in table 3, for copper B′ is the lower energy structure and *all atoms have positive definite moduli*. In contrast, in the B structure the moduli are non-positive definite for *six* atoms of which two possess non-strongly elliptic moduli. This is consistent with the results for the effective moduli shown in figure 8*a*, *b*. For the B structure C^*_{55} lies well above the upper bound and this suggests that this structure is not stable. Indeed, as mentioned in §2, the B structure in copper readily transforms into the B′ upon a small perturbation. Since for the B′ structure all atoms possess positive definite moduli, the Reuss lower bound, $\boldsymbol{C}_{\mathrm{R}}$, given by equation (3.12), can also be computed and it is shown as lower solid line in figure 8*b*. All bounds, $\boldsymbol{C}_{\mathrm{V}}$, $\boldsymbol{C}_{\mathrm{T}}$ and $\boldsymbol{C}_{\mathrm{R}}$ are rigorous in this case. The good agreement in this stable case between exact effective moduli from the discrete model and the continuum bounds is strong evidence that the continuum model of the boundary is justified. The fact that the exact modulus C_{44} only lies slightly below the lower bound indicates, nevertheless, that this boundary is stable and the continuum model is an approximate one. This latter observation is reasonable since the non-local natures of the atomic interactions are certainly not included in the local linear elasticity theory.

The two structures of the $\Sigma = 5$ (210) symmetrical tilt boundary have been carefully discussed so that the interpretation of other boundaries in terms of continuum properties of both the atomic level and effective moduli can be made. In

PHILOSOPHICAL TRANSACTIONS OF THE ROYAL SOCIETY A MATHEMATICAL, PHYSICAL & ENGINEERING SCIENCES

Figure 9

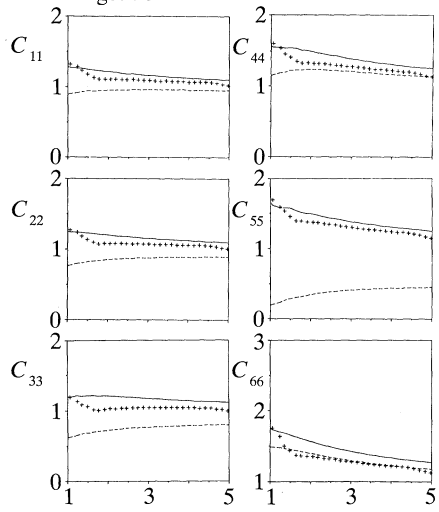

Figure 10

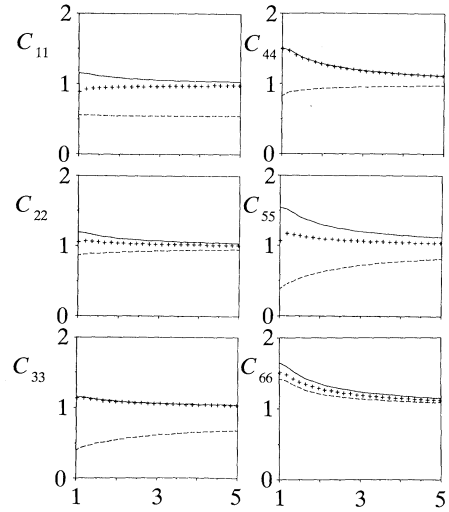

Figure 9. The effective moduli (points), the Voigt upper bound, $\boldsymbol{C}_{\mathrm{V}}$ (solid curve) and translation lower bound, $\boldsymbol{C}_{\mathrm{T}}$ (dashed curve) against the sub-block size h for the $\Sigma 13$ (320) symmetrical tilt boundary in gold, stable.

Figure 10. The effective moduli (points), the Voigt upper bound, $\boldsymbol{C}_{\mathrm{V}}$ (solid curve) and translation lower bound, $\boldsymbol{C}_{\mathrm{T}}$ (dashed curve) against the sub-block size h for the $\Sigma 13$ (510) symmetrical tilt boundary in gold, stable.

particular, the comparison of the exact effective moduli for the discrete model with the estimates from the continuum model can help to assess the stability of structures. Examples of stable and unstable structures were given above and an illustration of a metastable structure is given below for a $\Sigma = 5$ twist boundary.

Other symmetrical tilt boundaries in gold which have been studied are the $\Sigma = 5$ (310) boundary, two $\Sigma = 13$ boundaries with different misorientations and the $\Sigma = 73$ boundary. In the case of the $\Sigma = 5$ (310) boundary, corresponding to the C structure found in previous studies (Wang *et al.* 1984; Wang & Vitek 1986), the relaxation parts of the elastic moduli, $\tilde{\boldsymbol{C}}^{\alpha}$, are all negligible and thus the effective moduli are equal to the atomic level moduli $\bar{\boldsymbol{C}}^{\alpha}$. Hence, the exact effective moduli coincide in this case with the upper bound and the structure is stable. This is so although three atoms in the unit cell of this boundary possess non-positive definite moduli, one of which possess non-strongly elliptic moduli.

Figure 9 summarizes results for the $\Sigma = 13$ (320) boundary and figure 10 for the $\Sigma = 13$ (510) boundary. Following the structural unit model (Sutton & Vitek 1983) the repeat cell of the former boundary is composed of one B unit and one unit of the ideal crystal and the repeat cell of the latter boundary one C unit and two units of the ideal crystal. In both cases the exact effective moduli for the discrete system tend to lie between the bounds so that we characterize both structures as stable. Figure 11 gives similar results for the $\Sigma = 73$ (830) symmetrical tilt boundary the repeat cell of which is composed of one B unit and two C units. For this structure the moduli also lie between the bounds indicating that the structure is stable. These results are not surprising since the $\Sigma = 13$ and $\Sigma = 73$ boundaries are composed of the units of structures which are all stable and have well-behaved elastic moduli. The fact that the effective elastic properties for the discrete and continuum models are in better

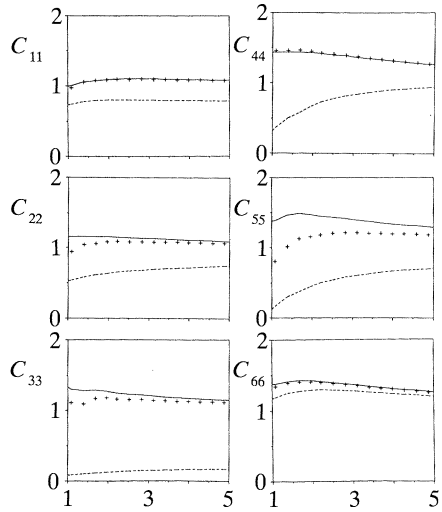

Figure 11. The effective moduli (points), the Voigt upper bound, $\boldsymbol{C}_{\mathrm{V}}$ (solid curve) and translation lower bound, $\boldsymbol{C}_{\mathrm{T}}$ (dashed curve) against the sub-block size h for the $\Sigma 73$ (830) symmetrical tilt boundary in gold, stable.

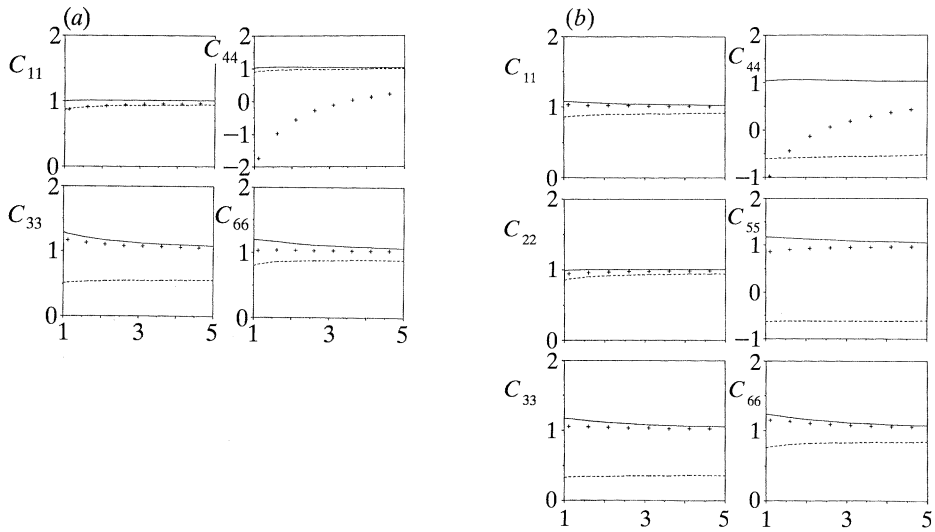

Figure 12. The effective moduli (points), the Voigt upper bound, $\boldsymbol{C}_{\mathrm{V}}$ (solid curve) and translation lower bound, $\boldsymbol{C}_{\mathrm{T}}$ (dashed curve) against the sub-block size h for the $\Sigma 5$ twist boundary in gold. (*a*) CSL structure, metastable; (*b*) type I structure, stable.

agreement for these longer period boundaries is further justification of the continuum analogue in general. In fact, when calculating the structures of short period boundaries, such as $\Sigma = 5$ (210), we are restricting the relaxations rather severely owing to the imposed short periodicity and thus it is more likely to encounter unstable or metastable structures. For example, additional relaxation, not allowed in the present calculations, may be a reconstruction leading to the increase in the size of the repeat cell. Indeed, it was shown in earlier pair-potential calculations that quadrupling the unit cell of the $\Sigma = 5$ (210) symmetrical tilt boundary leads to a new,

PHILOSOPHICAL TRANSACTIONS OF THE ROYAL SOCIETY A MATHEMATICAL, PHYSICAL & ENGINEERING SCIENCES

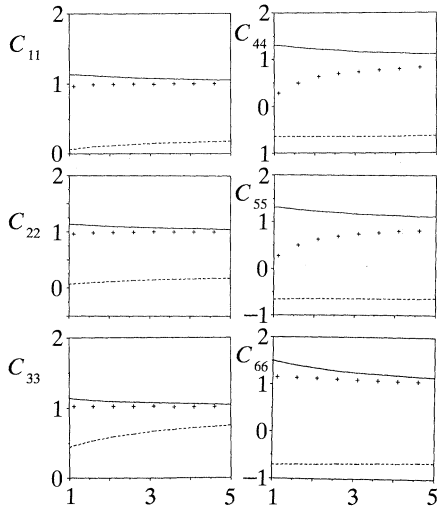

Figure 13. The effective moduli (points), the Voigt upper bound, $\boldsymbol{C}_{\mathrm{V}}$ (solid curve) and translation lower bound, $\boldsymbol{C}_{\mathrm{T}}$ (dashed curve) against the sub-block size h for the $\Sigma 13$ twist boundary in gold, stable.

energetically more favourable, structure (Vitek *et al.* 1985). A similar situation arises in the case of the $\Sigma = 5$ twist boundary as noted below.

The dependence of the effective moduli on the sub-block size h for the $\Sigma = 5$ twist boundary in gold is shown in figure 12*a*, *b* for the CSL and type I structures respectively. For the type I structure all the exact effective moduli for the discrete system lie between the bounds. Clearly, this is related to the fact that only four (two non-equivalent) atoms have non-positive definite moduli and none have any negative diagonal components of the tensor of moduli. This structure is clearly stable. On the other hand, in the CSL structure ten (three non-equivalent) atoms have non-positive definite moduli and two of them have negative shear modulus C_{44}. It is seen in figure 12*a* that the exact effective modulus C_{44} (and by symmetry also C_{55}) lies well below the lower bound and it is negative up to the distance of about 3.5 lattice spacings from the boundary. This implies that for the CSL structure the properties of the model of the boundary as a heterogeneous continuum do not approximate well the properties of the actual discrete system. This is an exception for the boundaries studied. However, the CSL structure is not unstable; it is a *metastable* higher energy structure which will transform to a lower energy one only if a sufficiently large perturbation is applied. None the less, the metastability of the CSL structure suggests that it may not be present in the bicrystals in spite of the fact that the observed structures show the CSL symmetry (Budai *et al.* 1983). More complex but more stable structures, corresponding to reconstructions into larger unit cells, may be present as suggested earlier by Oh & Vitek (1986).

Another twist boundary in gold which has been studied is the $\Sigma = 13$ boundary. Figure 13 summarizes the results for this boundary and shows that the exact effective moduli for the discrete system lie between the bounds so that the structure is stable. This is so in spite of the fact that following the structural unit model (Schwartz *et al.* 1985, 1988; Vitek 1988) the unit cell of this boundary is composed of one unit cell of the $\Sigma = 5$ boundary with the CSL structure and one unit of the ideal lattice. This emphasizes the specific peculiarity of the isolated CSL structure of the

$\Sigma = 5$ twist boundary which does not necessarily translate to the structures containing units of this boundary.

6. Conclusions

From the examples of both tilt and twist boundaries in bicrystals of gold and copper studied in this paper several important observations and conclusions emerge. In fact, many of these may be applicable to interfaces in bimaterials as well. First of all, the validity of a continuum model in which grain boundaries are regarded as heterogeneous media, where different phases are identified with individual atoms, is established. In this medium the elastic moduli of each phase, which occupies the interior of a Voronoi polyhedron, are identified with the second-order elastic constants associated with this atom. These atomic-level elastic constants vary considerably in the interface and are highly anisotropic due to irregular atomic structure. There are generally 21 distinct components of the modulus tensor $\boldsymbol{C}$ for atoms in the interface. While the tensor of elastic moduli associated with an atom in a perfect lattice is always positive definite, for atoms in the interface this may not be the case.

For bicrystals with stable grain boundary structures the majority of distinct atoms tend to have moduli which are positive definite or at least strongly elliptic. In this case elasticity BVPs for the associated continuum model are well posed, including the one that determines the effective properties of a heterogeneous medium. Grain boundaries with metastable and unstable structures tend to have a larger number of atoms for which the moduli are not positive definite or possibly not even strongly elliptic. Recall that positive definiteness is a requirement such that under all possible strain states the local strain energy is positive, while the weaker condition of strong ellipticity requires that waves propagate with real velocities.

For both the discrete atomistic structure and the heterogeneous continuum a natural and important problem arises concerning the effective moduli for the ensemble or block of atoms. These effective moduli characterize the response of the block to uniform external loading, for example a displacement corresponding to a uniform strain, as discussed in §3*c*. Whereas the effective moduli for the discrete system can be calculated exactly, as summarized in §4, those for the heterogeneous continuum cannot. Nevertheless, when the individual phases are all at least strongly elliptic rigorous bounds on the effective moduli for the continuum model can be obtained; otherwise we can only obtain estimates.

When the effective moduli of the bicrystal and the bounds are determined as functions of the distance from the boundary, as described in §5*b*, the exact effective moduli approach those of the ideal lattice at distances of order of ten lattice spacings. When all atoms or phases have positive definite moduli, as in the case of the B′ structure of the $\Sigma = 5$ (210) tilt boundary in copper, the agreement between the exact effective moduli for the discrete system and the bounds is very good even though the continuum model assumes only local elastic behaviour. As seen in several examples presented in §5, structures for which such an agreement is good are found to be stable. When some components of the exact effective moduli lie below the lower bound the corresponding structure is found to be metastable. Finally, when some components lie above the upper bound the structure is unstable. Hence the comparison between the atomistic and continuum predictions for the effective moduli proves to be a pertinent measure of the stability of a given structure.

PHILOSOPHICAL TRANSACTIONS OF THE ROYAL SOCIETY A MATHEMATICAL, PHYSICAL & ENGINEERING SCIENCES

The authors acknowledge very stimulating discussions with Professor P. Ponte-Castañeda and Professor J. R. Willis. This research was supported by the National Science Foundation under grant DMR 88-06966. The computations were performed at the computing facility of the Laboratory for Research on the Structure of Matter, University of Pennsylvania, supported by the National Science Foundation, MRL Program DMR 88-19885 and at the Pittsburgh Supercomputing Center.

Appendix A. Derivation of Francfort–Murat–Milton lower bound

Francfort & Murat (1986) introduced bounds on effective moduli for heterogeneous linear elastic solids based on the translation method, which relates to concepts of relative convexity discussed, for example, by Hill (1978, 1985). The following derivation most closely follows the recent work of Milton (1990). The BVP considers a heterogeneous elastic medium composed of N phases, where each phase occupies a region Ω_α

$$\sigma_{ij,j} = 0, \quad \text{in } \Omega_\alpha, \quad \alpha = 1, N, \tag{A 1a}$$

$$\sigma_{ij} = (C^\alpha - C^0)_{ijkl}\,\epsilon_{kl} = \Delta C^\alpha_{ijkl}\,\epsilon_{kl}, \quad \text{in } \Omega_\alpha, \quad \alpha = 1, N, \tag{A 1b}$$

with the displacement boundary conditions

$$u_k(\boldsymbol{x}) = \bar{\epsilon}_{kl}\,x_l, \quad \text{on} \quad S = S_\Omega \tag{A 1c}$$

and continuity of tractions and displacements is assumed across phase boundaries. The tensor of elastic moduli, $\boldsymbol{C}^\alpha$, in every phase α satisfies usual symmetry conditions

$$C^\alpha_{ijkl} = C^\alpha_{klij} = C^\alpha_{jikl}, \tag{A 2}$$

as does the translation operator $\boldsymbol{C}^0$ and also the moduli of the translated phases, hence $\Delta\boldsymbol{C}^\alpha$. In the original derivation $\boldsymbol{C}^\alpha$ is assumed to be positive definite for each phase.

Next we extend the translation method for constructing lower bounds to include strongly elliptic phases. In this case the following three requirements must hold. (i) $\boldsymbol{C}^\alpha$ must be semi-strongly elliptic, i.e.

$$C^\alpha_{ijkl}\,\xi_i\,\eta_j\,\xi_k\,\eta_l \geqslant 0 \tag{A 3}$$

for all vectors $\boldsymbol{\xi}$ and $\boldsymbol{\eta}$. (ii) The translation operator $\boldsymbol{C}^0$ must be quasi-convex, i.e.

$$\frac{1}{\Omega}\int_\Omega C^0_{ijkl}\,\epsilon_{ij}\,\epsilon_{kl}\,\mathrm{d}V \geqslant C^0_{ijkl}\,\bar{\epsilon}_{ij}\,\bar{\epsilon}_{kl}, \tag{A 4}$$

where $\bar{\boldsymbol{\varepsilon}}$ is defined by equation (3.8). (iii) ΔC^α_{ijkl}, defined in (A 1b), must be positive definite,

$$\Delta C^\alpha_{ijkl}\,\epsilon_{ij}\,\epsilon_{kl} > 0, \tag{A 5}$$

for all second-order tensors $\boldsymbol{\varepsilon}$. Consequently, the inverse tensor $(\Delta\boldsymbol{C}^\alpha)^{-1}$ is also positive definite, i.e.

$$(\Delta C^\alpha)^{-1}_{ijkl}\,\sigma_{ij}\,\sigma_{kl} > 0 \tag{A 6}$$

for all second-order tensors $\boldsymbol{\sigma}$.

By definition of effective constants for the heterogeneous material with phases ΔC^α_{ijkl} we have

$$\Delta C^*_{ijkl}\,\bar{\epsilon}_{ij}\,\bar{\epsilon}_{kl} \equiv 2W_\Delta, \tag{A 7}$$

where W_Δ is the strain-energy density corresponding to the actual solution for the

translated material and the average of actual strain is defined as $\bar{e}_{ij} = 1/\Omega \int_\Omega e_{ij}\,\mathrm{d}V$; also $[\Delta C^{-1}]^*_{ijkl} \equiv [\Delta C^*]^{-1}_{ijkl}$.

Next, from the condition of positive definiteness of $(\Delta \boldsymbol{C}^\alpha)^{-1}$ it follows that we can use the minimum complementary energy theorem, which for displacement boundary conditions has the form

$$-2W_\Delta = \min\left\{\frac{1}{\Omega}\sum_{\alpha=1}^{N}\int_{\Omega_\alpha}(\Delta C^\alpha)^{-1}_{ijkl}\,\tilde{\sigma}_{ij}\,\tilde{\sigma}_{kl}\,\mathrm{d}V - \frac{2}{\Omega}\int_S n_i\,\tilde{\sigma}_{ij}\,u_j\,\mathrm{d}S\right\} \tag{A 8}$$

among all self-equilibrated stress fields $\tilde{\boldsymbol{\sigma}}$. For constant trial fields $\tilde{\boldsymbol{\sigma}}$ the previous expression can be rewritten in the form

$$-\left[\sum_{\alpha=1}^{N}\left(\frac{\Omega_\alpha}{\Omega}\right)(\Delta C^\alpha)^{-1}_{ijkl}\right]\tilde{\sigma}_{ij}\,\tilde{\sigma}_{kl} + 2\tilde{\sigma}_{ij}\,\bar{e}_{ij} \leqslant 2W_\Delta. \tag{A 9}$$

To get an optimal lower bound on $2W_\Delta$ we take the derivative of the left-hand side with respect to $\tilde{\boldsymbol{\sigma}}$ to get

$$\left[\sum_{\alpha=1}^{N}\left(\frac{\Omega_\alpha}{\Omega}\right)(\Delta C^\alpha)^{-1}_{ijkl}\right]\tilde{\sigma}_{kl} = \bar{e}_{ij} \tag{A 10}$$

or

$$\tilde{\sigma}_{ij} = \left[\sum_{\alpha=1}^{N}\left(\frac{\Omega_\alpha}{\Omega}\right)(\Delta C^\alpha)^{-1}\right]^{-1}_{ijkl}\bar{e}_{kl}. \tag{A 11}$$

Substituting (A 10) and (A 11) into (A 9) we get a lower bound on the strain energy of the translated material

$$\left[\sum_{\alpha=1}^{N}\left(\frac{\Omega_\alpha}{\Omega}\right)(\Delta C^\alpha)^{-1}\right]^{-1}_{ijkl}\bar{e}_{ij}\,\bar{e}_{kl} \leqslant 2W_\Delta. \tag{A 12}$$

The condition of positive definiteness of $\Delta \boldsymbol{C}^\alpha$ ensures the validity of the theorem of minimum potential energy, which for displacement boundary conditions gives

$$2W_\Delta = \min\left(\frac{1}{\Omega}\sum_{\alpha=1}^{N}\int_{\Omega_\alpha}\Delta C^\alpha_{ijkl}\,\tilde{e}_{ij}\,\tilde{e}_{kl}\,\mathrm{d}V\right) \tag{A 13}$$

among all fields such that $1/\Omega\int_\Omega \tilde{e}_{ij}\,\mathrm{d}V = \bar{e}_{ij}$ and $u_k(s) = \bar{e}_{kl}\,x_l$. Thus from (A 12) and (A 13) with (A 1*b*)

$$\left[\sum_{\alpha=1}^{N}\left(\frac{V_\alpha}{V}\right)(\Delta C^\alpha)^{-1}\right]^{-1}_{ijkl}\bar{e}_{ij}\,\bar{e}_{kl} \leqslant \min\left[\frac{1}{\Omega}\sum_{\alpha=1}^{N}\int_{\Omega_\alpha}C^\alpha_{ijkl}\,\tilde{e}_{ij}\,\tilde{e}_{kl}\,\mathrm{d}V - \frac{1}{\Omega}\int_\Omega C^0_{ijkl}\,\tilde{e}_{ij}\,\tilde{e}_{kl}\,\mathrm{d}V\right]. \tag{A 14}$$

Hence, with (A 4) and (A 14) it follows that

$$\left[\sum_{\alpha=1}^{N}\left(\frac{V_\alpha}{V}\right)(\Delta C^\alpha)^{-1}\right]^{-1}_{ijkl}\bar{e}_{ij}\,\bar{e}_{kl} \leqslant \min\left[\frac{1}{\Omega}\sum_{\alpha=1}^{N}\int_{\Omega_\alpha}C^\alpha_{ijkl}\,\tilde{e}_{ij}\,\tilde{e}_{kl}\,\mathrm{d}V\right] - C^0_{ijkl}\,\bar{e}_{ij}\,\bar{e}_{kl}. \tag{A 15}$$

By definition of effective elastic constants for actual (non-translated) heterogeneous medium

$$C^*_{ijkl}\,\bar{e}_{ij}\,\bar{e}_{kl} \equiv 2W \tag{A 16}$$

and substitution into (A 14) yields

$$(C_{\mathrm{T}})_{ijkl}\,\bar{\epsilon}_{ij}\,\bar{\epsilon}_{kl} \equiv \left\{\left[\sum_{\alpha=1}^{N}\left(\frac{V_\alpha}{V}\right)(\Delta C^\alpha)^{-1}\right]^{-1}_{ijkl} + C^0_{ijkl}\right\}\bar{\epsilon}_{ij}\,\bar{\epsilon}_{kl}$$
$$\leqslant \min\left[\frac{1}{\Omega}\sum_{\alpha=1}^{N}\int_{\Omega_\alpha} C^\alpha_{ijkl}\,\tilde{\epsilon}_{ij}\,\tilde{\epsilon}_{kl}\,\mathrm{d}V\right] \equiv C^*_{ijkl}\,\bar{\epsilon}_{ij}\,\bar{\epsilon}_{kl}. \quad \text{(A 17)}$$

Finally, to illustrate the importance of conditions (i)–(iii) we note the following. (*a*) If the condition (iii) for positive definiteness of $\Delta\boldsymbol{C}^\alpha$ fails, but (i) and (ii) are satisfied, then the basic inequality fails and so does the lower bound. (*b*) If condition (ii) for quasi-convexity of $\boldsymbol{C}^0$ fails, while other conditions are valid, then there is lower bound on $\Delta\boldsymbol{C}^\alpha$, but we cannot extract an exact lower bound on $\boldsymbol{C}^*$. (*c*) If the condition (i) is not satisfied (for example $C^\alpha_{1212} < 0$ and phase α is not semi-strongly elliptic). It can be proven that there does not exist minimum for potential energy for such phase. The latter two cases arise in the examples considered in this paper and, therefore, we regard $\boldsymbol{C}_{\mathrm{T}}$ in such cases as an estimate rather than a bound.

Appendix B. Effective elastic moduli in discrete periodic structures

Let us consider a periodic structure the unit cell of which contains N non-equivalent atoms and associate each of these atoms with a different sublattice; indices denoting individual sublattices are $p(\alpha), \alpha = 1, \ldots, N$. We now apply to this structure a macroscopically homogeneous strain $\boldsymbol{\varepsilon}$ related to the deformation gradient, $\boldsymbol{F}$, according to equation (3.2). On the microscopic level this strain does not induce a homogeneous displacement of all the atoms but different sublattices will be displaced differently with respect to each other (Born & Huang 1954; Martin 1975*b*). Let $\boldsymbol{R}^{\alpha\beta}$ be the vector connecting atoms α and β, belonging to sublattices $p(\alpha)$ and $p(\beta)$, respectively, in the undeformed state, and $\boldsymbol{r}^{\alpha\beta}$ is the vector connecting the same atoms in the deformed state. This vector can be expressed as

$$\boldsymbol{r}^{\alpha\beta} = \boldsymbol{F}\boldsymbol{R}^{\alpha\beta} + \boldsymbol{\delta}^{p(\beta)} - \boldsymbol{\delta}^{p(\alpha)}, \quad \text{(B 1)}$$

where $\boldsymbol{\delta}^p$ is the internal displacement vector of the sublattice p relative to a reference sublattice, for example $p(1)$. It is convenient to transform the internal displacement vectors to a rotationally invariant set of $N-1$ independent vectors $\boldsymbol{\zeta}^p$ defined by the relation:

$$\boldsymbol{\zeta}^p = \boldsymbol{F}^T\boldsymbol{\delta}^p, \quad \text{(B 2)}$$

where $\boldsymbol{F}^T$ is the transpose of the deformation gradient $\boldsymbol{F}$. It has been shown by Martin (1975*b*) that the formulas for stresses and elastic moduli take then simple forms when expressed in terms of the square of the distance between atoms α and β, $s^{\alpha\beta} = \boldsymbol{r}^{\alpha\beta}\boldsymbol{r}^{\alpha\beta}$. By using equations (B 1) and (B 2) we obtain for the lagrangian strain defined by equation (3.2)

$$s^{\alpha\beta} = \boldsymbol{R}^{\alpha\beta}(2\boldsymbol{\varepsilon}+\boldsymbol{I})\,\boldsymbol{R}^{\alpha\beta} + 2(\boldsymbol{\zeta}^{p(\beta)}-\boldsymbol{\zeta}^{p(\alpha)})\,\boldsymbol{R}^{\alpha\beta} + (\boldsymbol{\zeta}^{p(\beta)}-\boldsymbol{\zeta}^{p(\alpha)})\,(2\boldsymbol{\varepsilon}+\boldsymbol{I})^{-1}\,(\boldsymbol{\zeta}^{p(\beta)}-\boldsymbol{\zeta}^{p(\alpha)}). \quad \text{(B 3)}$$

Assuming that the atomic interactions are given by many-body potentials of the type (2.1), then using equation (4.2) the atomic level stress associated with an atom α is

$$\sigma^\alpha_{ij} = \frac{1}{\Omega^\alpha}\left[\sum_\beta V'(s^{\alpha\beta}) - 2f'(\rho^\alpha)\sum_\beta \Phi'(s^{\alpha\beta})\right]R^{\alpha\beta}_i\,R^{\alpha\beta}_j, \quad \text{(B 4)}$$

where the derivatives of V and Φ are taken with respect to $s^{\alpha\beta}$. The atomic level elastic moduli associated with an atom α, defined by equation (4.3), are then

$$C^{\alpha}_{ijkl} = \frac{4}{\Omega}\Big\{\sum_{\beta}[\tfrac{1}{2}V''(s^{\alpha\beta}) - f'(\rho_\alpha)\,\Phi''(s^{\alpha\beta})]\,R^{\alpha\beta}_i R^{\alpha\beta}_j R^{\alpha\beta}_k R^{\alpha\beta}_l - f''(\rho_\alpha)\sum_{\gamma}\Phi'(s^{\alpha\gamma})\,R^{\alpha\gamma}_i R^{\alpha\gamma}_j \sum_{\beta}\Phi'(s^{\alpha\beta})\,R^{\alpha\beta}_k R^{\alpha\beta}_l\Big]. \quad \text{(B 5)}$$

The relaxation part of the elastic moduli is given by equation (4.5) in terms of D^{α}_{ijn} and $E^{\alpha\beta}_{pq}$. Substituting (2.1) into equations (4.6a, b) gives:

$$D^{\alpha}_{ijn} = 2\,(DV^{\alpha}_{ijn} - 2DN^{\alpha}_{ijn}) \quad \text{(B 6}a\text{)}$$

and

$$E^{\alpha\beta}_{pq} = \sum_{\gamma,\delta}\{[2V''(s^{\gamma\delta}) - 4f'(\rho_\gamma)\,\Phi''(s^{\gamma\delta})]\,R^{\gamma\delta}_p R^{\gamma\delta}_q\,\delta_{\beta\delta,\,\beta\gamma}\,\delta_{\alpha\delta,\,\alpha\gamma} + [V'(s^{\gamma\delta}) - 2f'(\rho_\gamma)\,\Phi'(s^{\gamma\delta})]\,\delta_{pq}\,\delta_{\beta\delta,\,\beta\gamma}\,\delta_{\alpha\delta,\,\alpha\gamma}\} - 4\sum_{\gamma} f''(\rho_\gamma)\sum_{\kappa}\Phi'(s^{\gamma\kappa})\,R^{\gamma\kappa}_q\,\delta_{\beta\kappa,\,\beta\gamma}\sum_{\delta}\Phi'(s^{\gamma\delta})\,R^{\gamma\delta}_p\,\delta_{\alpha\delta,\,\alpha\gamma}, \quad \text{(B 6}b\text{)}$$

where

$$DV^{\alpha}_{ijn} = \sum_{\beta,\gamma}[V''(s^{\beta\gamma}) - 2f'(\rho_\beta)\,\Phi''(s^{\beta\gamma})]\,R^{\beta\gamma}_i R^{\beta\gamma}_j R^{\beta\gamma}_n\,\delta_{\alpha\gamma,\,\alpha\beta}$$

$$DN^{\alpha}_{ijn} = \sum_{\beta} f''(\rho_\beta)\Big[\sum_{\gamma=1}^{N}\Phi'(s^{\beta\gamma})\,R^{\beta\gamma}_i\,\delta_{\alpha\gamma,\,\alpha\beta}\Big(\sum_{\delta}\Phi'(s^{\alpha\delta})\,R^{\alpha\delta}_j R^{\alpha\delta}_n\Big)\Big]$$

and

$$\delta_{\alpha\gamma,\,\alpha\beta} = \{\delta[p(\alpha) - p(\gamma)] - \delta[p(\alpha) - p(\beta)]\}.$$

The procedure described in this Appendix and in §4 allows us to evaluate exactly the effective moduli for any three-dimensionally periodic structure. However, in the atomistic calculations of grain boundaries only two-dimensional periodicity, in the plane parallel to the boundary, is imposed while in the direction perpendicular to the boundary the block is effectively infinite (see §2). Hence, when evaluating the relaxation part of the effective moduli, $\tilde{C}_{ijkl}$, the following procedure was adopted. For each relaxed structure a periodic array of grain boundaries was constructed such that individual grain boundaries are separated to such an extent that no interaction between them occurs. This construction is purely geometrical and no additional relaxation of atomic positions has been allowed. By using the boundary periodicity and periodicity of the array of boundaries, a three-dimensional repeat cell can easily be defined. It contains two, well separated, boundaries. However, most of the atoms in this cell are far away from the boundary, in the region of the ideal lattice. In particular, we regarded any atom at the distance bigger than twice the largest repeat vector in the boundary plane, as being in the ideal lattice. This is a reasonable assumption since the strain field associated with grain boundaries decreases rapidly and becomes negligible at this distance (Read & Shockley 1953; Hirth & Lothe 1982). For such an atom α both D^{α}_{ijn} and $E^{\alpha\beta}_{pq}$ have then been put equal to zero. This reduces substantially the number of linear equations in the set (4.6c) and makes the problem more tractable.

References

Ackland, G. J. & Finnis, M. W. 1986 *Phil. Mag.* A **54**, 301.

Ackland, G. J., Finnis, M. W. & Vitek, V. 1988 *J. Phys.* F **18**, L 153.

Ackland, G. J., Tichy, G., Vitek, V. & Finnis, M. W. 1987 *Phil. Mag* A **56**, 735.

Adams, J. B., Wolfer, W. G. & Foiles, S. M. 1989 *Phys. Rev.* B **40**, 7479.

Aucouturier, M. (ed.) 1990 Intergranular and interphase boundaries in materials. *J. Phys. Fr.* **51**, C1.

Balluffi, R. W. 1986 Grain boundary structure and related phenomena. *Trans. Jap. Inst. Metals* **27**, 23.

Balluffi, R. W., Rühle, M. & Sutton, A. P. 1987 *Mater. Sci. Engng* **89**, 1.

Bassani, J. L. & Qu, J. 1990 *Metal-ceramic interfaces* (ed. M. Rühle, A. G. Evans, M. F. Ashby & J. P. Hirth). Oxford: Pergamon Press.

Born, M. & Huang, K. 1954 *Dynamical theory of crystal lattices.* Oxford: Clarendon Press.

Bristowe, P. D. 1986 Grain boundary structure and related phenomena. *Trans. Jap. Inst. Metals* **27**, 89.

Bristowe, P. D. & Crocker, A. G. 1978 *Phil. Mag.* A **38**, 487.

Budai, J., Bristowe, P. D. & Sass, S. L. 1983 *Acta metall.* **31**, 699.

Chen, S. P., Egami, T. & Vitek, V. 1988 *Phys. Rev.* B **37**, 2440.

Daw, M. S. & Baskes, M. I. 1983 *Phys. Rev. Lett.* **50**, 1285.

Daw, M. S. & Baskes, M. I. 1984 *Phys. Rev.* B **29**, 6443.

Finnis, M. W. & Sinclair, J. E. 1984 *Phil. Mag.* A **50**, 45.

Francfort, G. A. & Murat, F. 1986 Homogenization and optimal bounds in linear elasticity. *Arch. ration. Mech. Analysis* **94**, 307.

Gurtin, M. E. 1963 *Q. Jl appl. Math.* **20**, 379.

Hashin, Z. 1983 *J. appl. Mech.* **50**, 481.

Hill, R. 1968 *J. Mech. Phys. Solids* **16**, 229, 315.

Hill, R. 1978 *Adv. Sol. Mech.* **18**, 1.

Hill, R. 1985 *Math. Proc. Camb. phil. Soc.* **98**, 579.

Hirth, J. P. & Lothe, J. 1982 *Theory of dislocations.* New York: Wiley-Interscience.

Ishida, Y. (ed.) 1986 Grain boundary structure and related phenomena. *Trans. Jap. Inst. Metals* **27**.

Johnson, R. A. 1988 *Phys. Rev.* B **37**, 3924.

Kittel, C. 1986 *Introduction to solid state physics.* New York: John Wiley.

Knops, R. J. & Payne, L. E. 1971 *Uniqueness theorems in linear elasticity*, vol. 19. New York: Springer.

Maradudin, A. A., Montroll, E. W., Weiss, G. H. & Ipatova, I. P. 1971 In *Solid state physics* (ed. H. Ehrenreich, F. Seitz & D. Turnbull), suppl. 3. New York: Academic Press.

Martin, J. W. 1975*a* *J. Phys.* C **8**, 2837.

Martin, J. W. 1975*b* *J. Phys.* C **8**, 2858.

Mehrabadi, M. M. & Nemat-Nasser, S. 1987 *Mech. Mater.* **6**, 127.

Milton, G. W. 1990 *Comm. pure appl. Math.* **43**, 63.

Milton, G. W. & Kohn, R. V. 1988 *J. Mech. Phys. Solids* **36**, 6, 397.

Oh, Y. & Vitek, V. 1986 *Acta metall.* **34**, 1941.

Pond, R. C. & Bollmann, W. 1979 *Phil. Trans. R. Soc. Lond.* A **292**, 449.

Raj, R. & Sass, S. L. (eds) 1988 Interface science and engineering '87. *J. Phys. Paris* **49**, C5.

Rapaport, D. C. 1988 *Comp. Phys. Rep.* **9**, 1.

Read, W. T. & Shockley, W. 1950 *Phys. Rev.* **78**, 275.

Rühle, M., Evans, A. G., Ashby, M. F. & Hirth, J. P. (eds) 1990 *Metal-ceramic interfaces.* Oxford: Pergamon Press.

Schwartz, D., Vitek, V. & Sutton, A. P. 1985 *Phil. Mag.* A **51**, 499.

PHILOSOPHICAL TRANSACTIONS OF THE ROYAL SOCIETY A MATHEMATICAL, PHYSICAL & ENGINEERING SCIENCES

Schwartz, D., Bristowe, P. D. & Vitek, V. 1988 *Acta metall.* **36**, 675.

Srolovitz, D. J., Maeda, K., Vitek, V. & Egami, T. 1981 *Phil. Mag.* A **44**, 847.

Sutton, A. P. 1984 *Int. Metals Rev.* **29**, 377.

Sutton, A. P. & Vitek, V. 1983 *Phil. Trans. R. Soc. Lond.* A **309**, 1.

Tersoff, J., Vanderbilt, D. & Vitek, V. (eds) 1989 *Atomic scale calculations in materials science*, vol. 141. Pittsburgh: Materials Research Society.

Vitek, V. 1984 *Dislocations 1984* (ed. P. Veyssière, L. Kubin & J. Castaign), p. 435. Paris: Editions CNRS.

Vitek, V. 1988 *J. Phys. Paris* **49**, C5–115.

Vitek, V. & Egami, T. 1987 *Phys. Stat. Sol.* (b) **144**, 145.

Vitek, V., Minonishi, Y. & Wang, G. J. 1985 *J. Phys. Paris* **46**, C4–171.

Vitek, V. & Srolovitz, D. J. (eds) 1989 *Atomistic simulation of materials: beyond pair potentials.* New York: Plenum Press.

Vitek, V., Sutton, A. P., Smith, D. A. & Pond, R. C. 1979 In *Grain boundary structure and kinetics* (ed. R. W. Balluffi), p. 115. Metals Park, Ohio: ASM.

Walpole, L. J. 1983 *Adv. appl. Mech.* **21**, 169.

Wang, G. J. & Vitek, V. 1986 *Acta metall.* **34**, 951.

Wang, G. J., Sutton, A. P. & Vitek, V. 1984 *Acta metall.* **32**, 1093.

Willis, J. R. 1981 *Adv. appl. Mech.* **21**, 1.

Willis, J. R. 1983 *J. appl. Mech.* **50**, 1202.

Wolf, D. & Kluge, M. 1990 *Scripta metall.* **24**, 907.

Wolf, D. & Lutsko, J. F. 1989 J. mater. Res. **4**, 1427.

Wolf, D., Lutsko, J. F. & Kluge, M. 1989 In *Atomistic simulation of materials: beyond pair potentials* (ed. V. Vitek & D. J. Srolovitz), p. 245. New York: Plenum Press.

Yoo, M. H., Clark, W. A. T. & Briant, C. L. (eds) 1988 *Interfacial structure, properties and design*, vol. 122. Pittsburgh: Materials Research Society).

Received 2 May 1991; accepted 10 September 1991

PHILOSOPHICAL TRANSACTIONS OF THE ROYAL SOCIETY A MATHEMATICAL, PHYSICAL & ENGINEERING SCIENCES